Classical lumps and their quantum descendents in the Regge limit of QCD

Raju Venugopalan

Brookhaven National Laboratory

Cracow School of Theoretical Physics, Zakopane, 2021

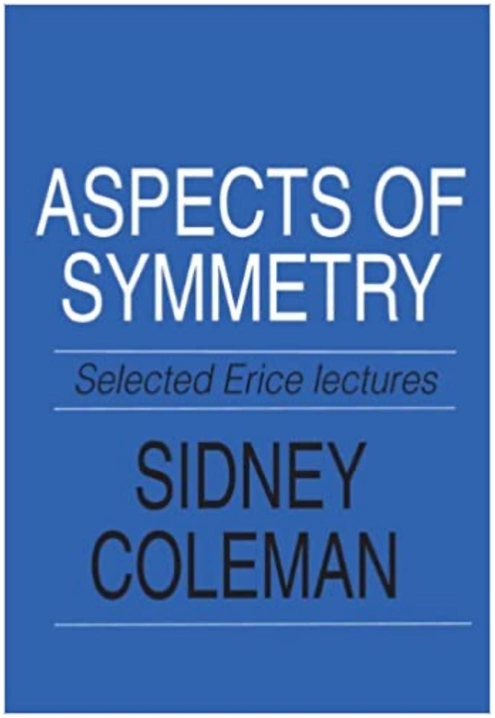

“Classical lumps and their quantum descendents”

Landscape of scattering in the strong interaction

Aschenauer et al., arXiv:1708.01527
Rep.Prog. Phys. 82, 024301 (2019)

A perspective from the Resolution-Energy plane

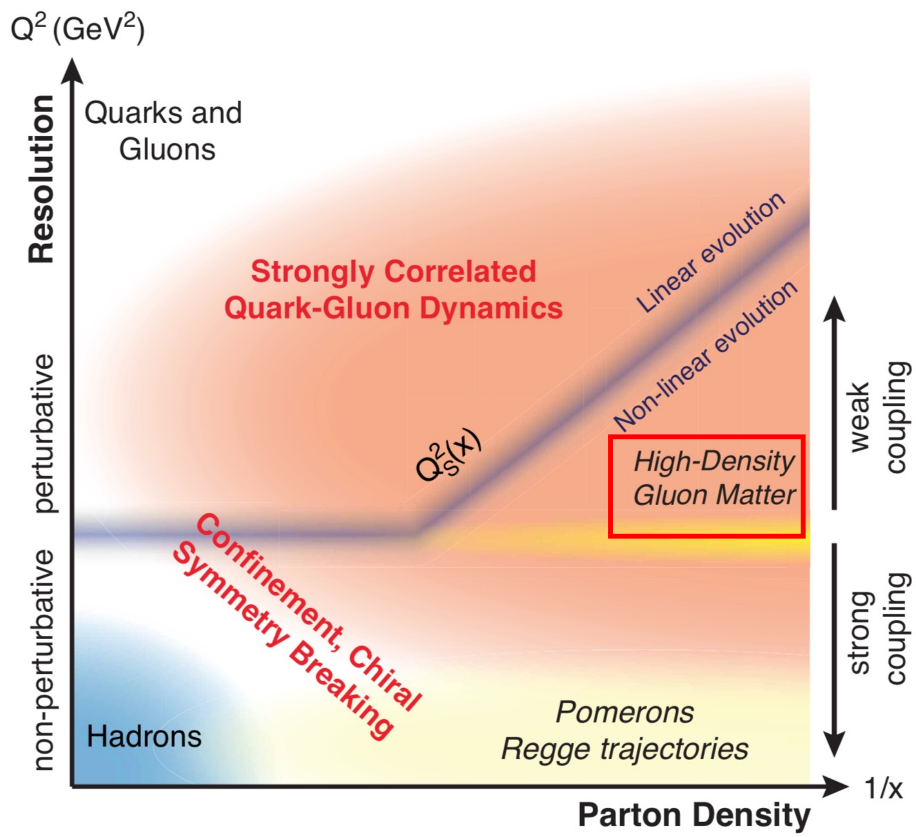

Many open questions: three-D structure, spin and orbital dynamics, many-body correlations, multi-particle production

The proton as a complex many-body system

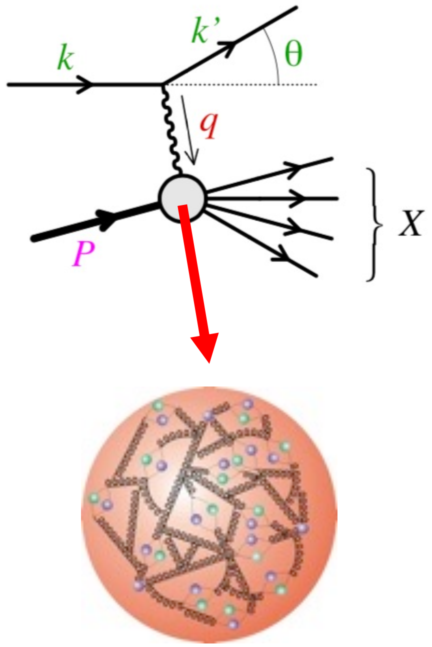

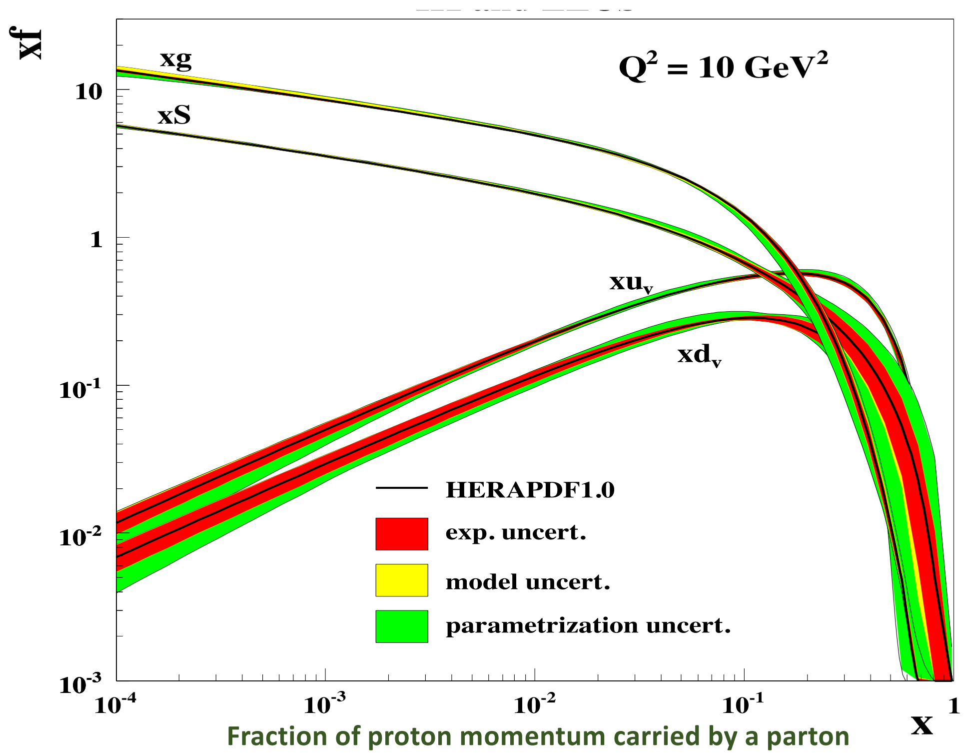

A key lesson from the HERA DIS collider:

Gluons and sea quarks dominate the proton wave-function at high energies

Lifting the veil: boosting the proton uncovers many-body structure

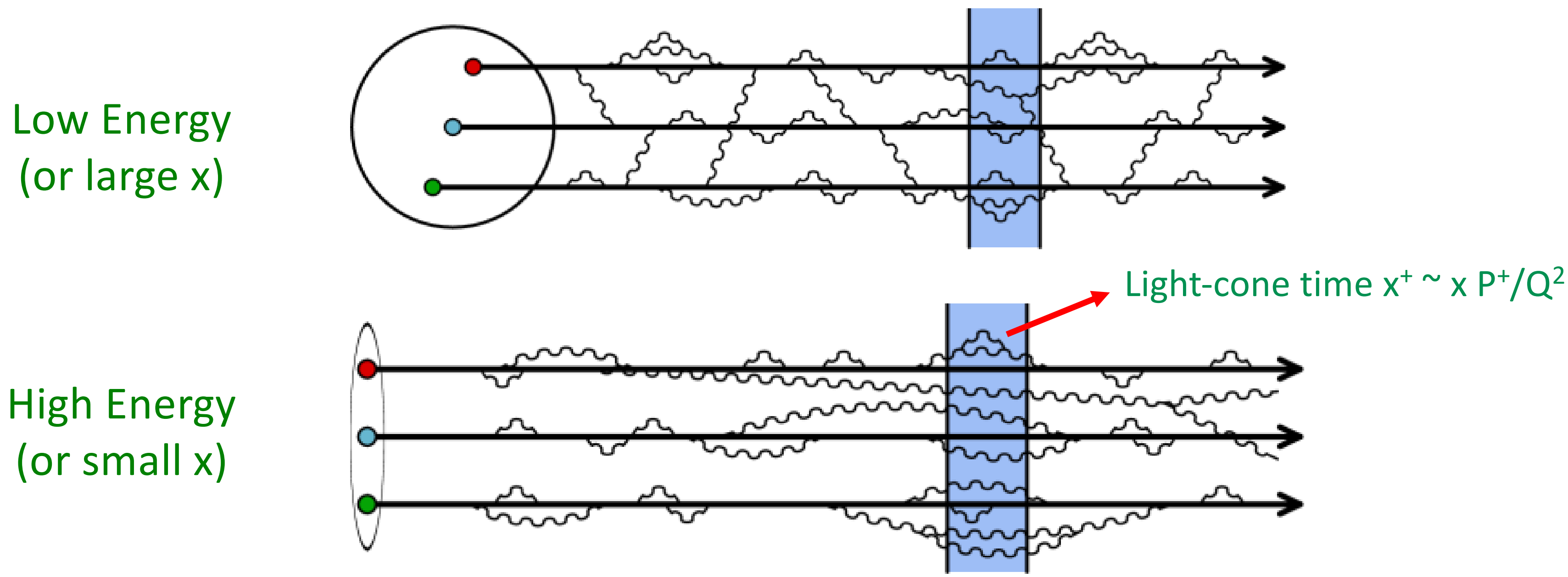

Wee parton fluctuations time dilated on strong interaction time scales.

Long lived gluons radiate further small x gluons…Markovian process generates power law growth of gluon distribution at small x

Generating strong fields by multiparticle production

Multiparticle production in the Regge limit:

$s \to \infty, Q^2 = \text{fixed} \gg \Lambda^2_{QCD}, \text{x} \to 0$

A fascinating equilibrium of splitting and recombination should eventually result. It is a considerable theoretical challenge to calculate this equilibrium in detail…

F. Wilczek, Nature (1999)

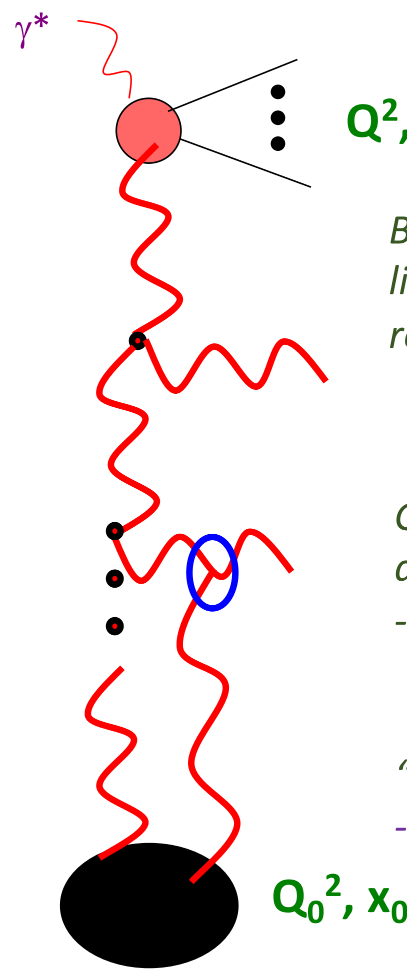

Bremsstrahlung
linear QCD evolution
resums large logs in x: BFKL

Gluon recombination
and screening
- non-linear QCD evolution

"all twist" $(1/Q^2)^n$ terms
"death by a million cuts"
- challenging for pQCD

The boosted proton

Gluon saturation = Classicalization

Gribov,Levin,Ryskin (1983)
Mueller, Qiu (1986)

Decoupling of longitudinal
and transverse dynamics
In the hadron infinite momentum frame

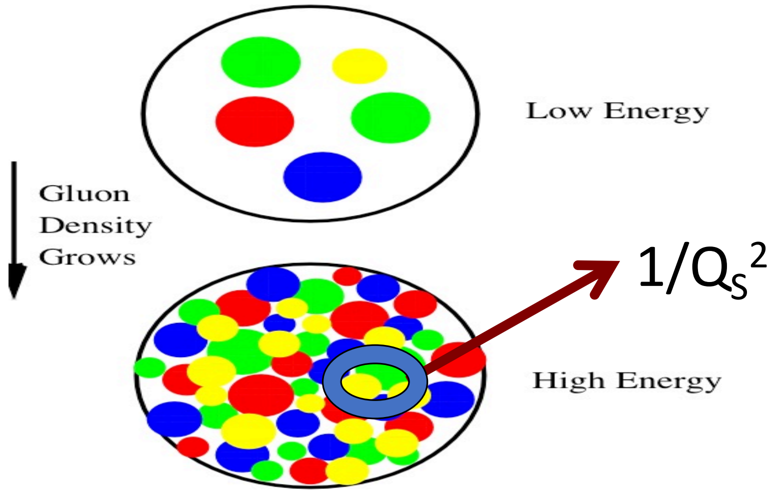

Gluon saturation:

Gluons at maximal phase space occupancy $n = \frac{1}{\alpha_S}$

resist further close packing by recombining and screening their color charges

Emergent dynamical saturation scale $Q_S(x) >> \Lambda_{QCD}$ Asymptotic freedom! $\alpha_S(Q_S) << 1$

Large phase space occupancy leads to classicalization

McLerran,RV (1994)

Saturation as perturbative unitarization: the dipole model

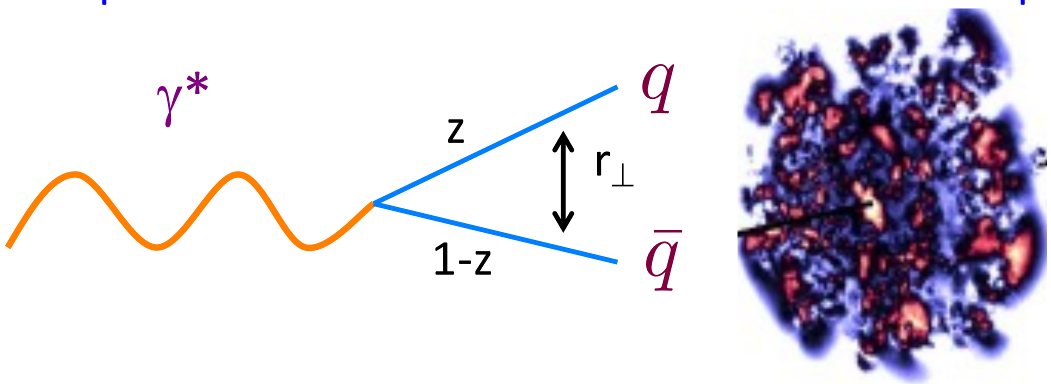

$$\sigma_{\mathrm{T,L}}^{\gamma^*,P} = \int d^2 r_\perp \int dz \, |\psi_{\mathrm{T,L}}(r_\perp, z, Q^2)|^2 \, \sigma_{q,\bar{q},P}(r_\perp, x)$$

QED QCD

$$\sigma_{q\bar{q}P}(r_\perp, x) = \sigma_0 \left[1 - \exp\left(-r_\perp^2 \, Q_s^2(x)\right)\right]$$

Golec-Biernat Wusthoff model

$$\boxed{Q_s^2(x) = Q_0^2 \left(\frac{x_0}{x}\right)^\lambda}$$

Parameters from HERA fit:
Q_0 = 1 GeV; λ = 0.3;
x_0 = 3* 10^{-4}; σ_0 = 23 mb

Color transparency of S-matrix for $r_\perp^2 Q_S^2$ << 1 ($\sigma \propto A$)

Color opacity (”black disk”) of S-matrix for $r_\perp^2 Q_S^2$ >> 1 ($\sigma \propto A^{2/3}$)

QCD picture of “shadowing”…

Geometrical scaling: evidence for Q_S?

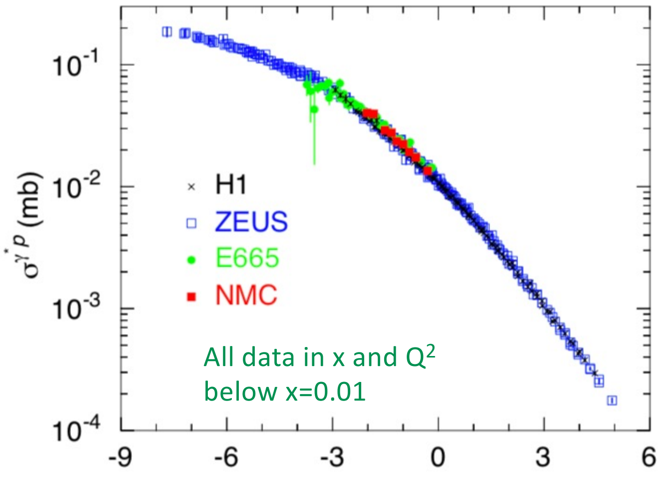

Q^2/Q_S^2

Original observation by
Stasto, Golec-Biernat and Kwiecinski, PRL (2001)

Plot from Gelis, Peschanski, Soyez, Schoeffel, PLB (2007)

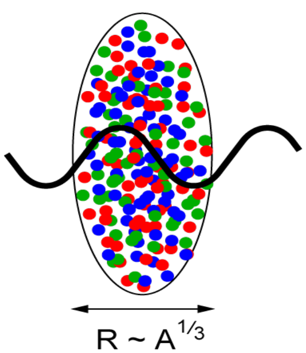

$Q_S^2 \sim A^{1/3}$ since "wee" gluons couple coherently for $x << A^{-1/3}$

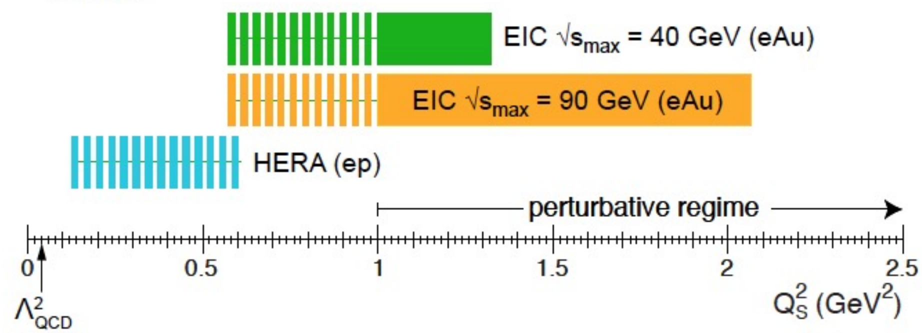

Big nuclear "oomph" in Q_S at the future Electron-Ion Collider

"Mining for gluon saturation at colliders"
A. Morreale and F. Salazar, 2108.08254 [hep-ph]

Classicalization and perturbative unitarization

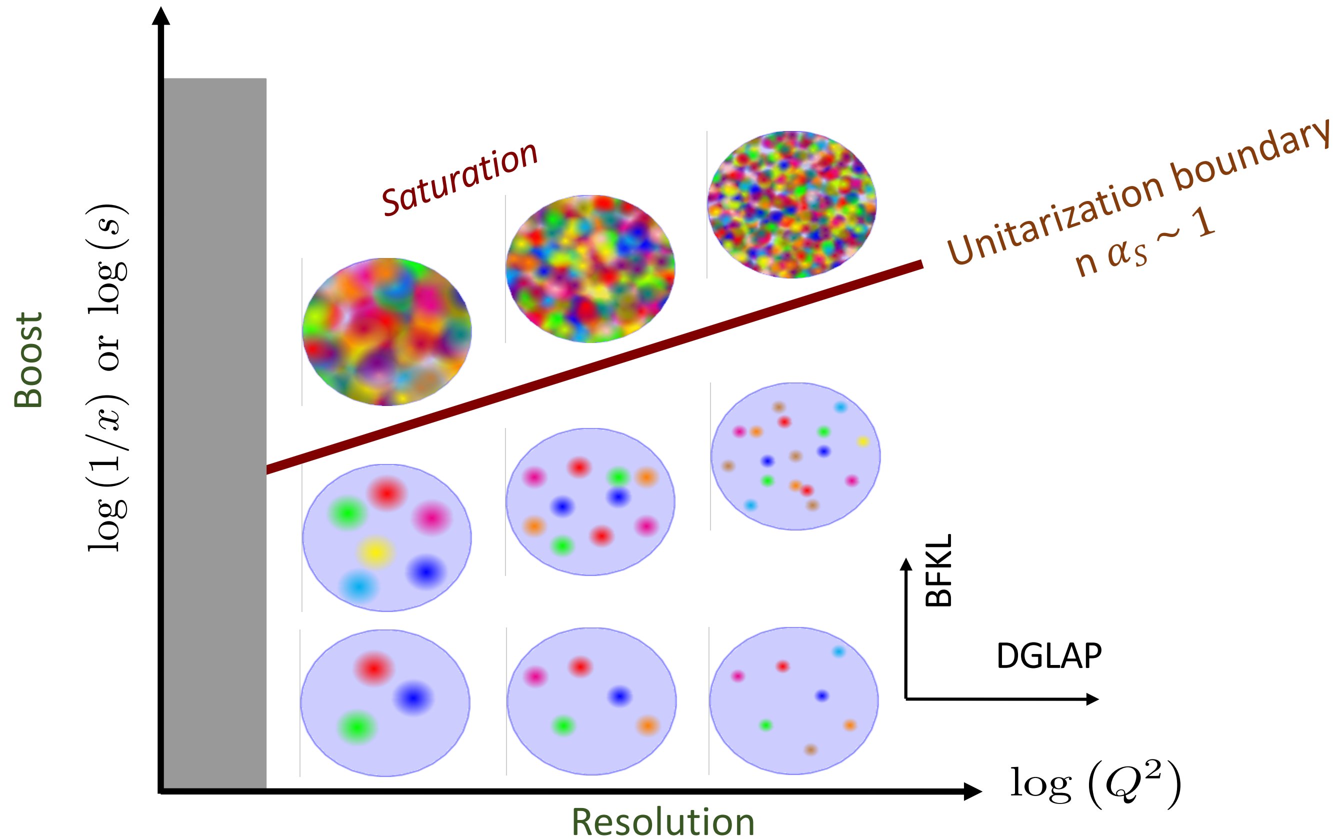

Classicalization and perturbative unitarization tied together by the emergent saturation scale $Q_S(x)$

An analogous phenomenon may occur in trans-Planckian scattering of gravitons resulting in a Black Hole

Dvali, Gomez (2010)

EFT describing saturation and unitarization: the Color Glass Condensate

Born-Oppenheimer separation between fast and slow modes

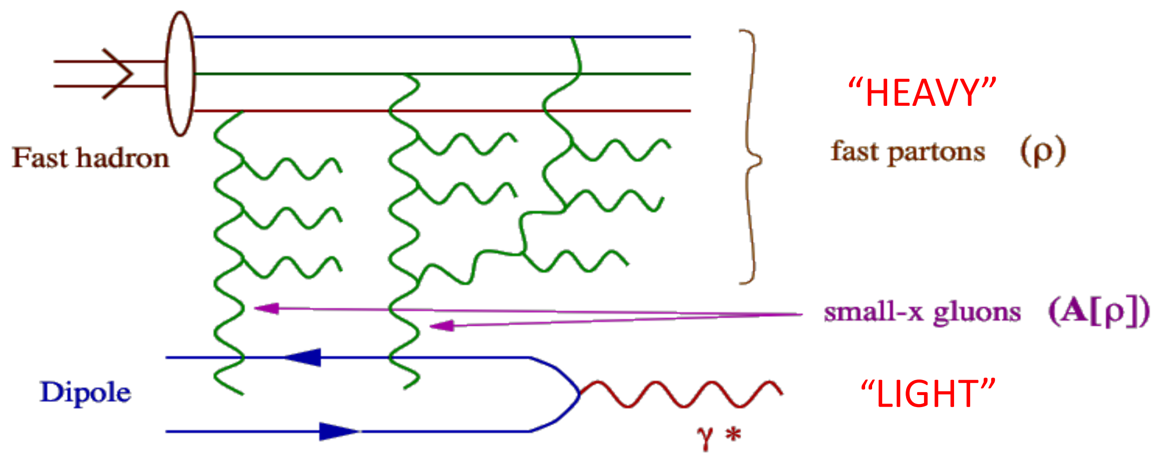

CGC: Effective Field Theory of classical static parton sources and dynamical gluon fields

McLerran, RV (1994)
Iancu,Leonidov, McLerran (2001)

Color: self-evident
Glass: stochastic dynamics of static sources
Condensate: Highly occupied fields form a condensate in presence of color sources, on time scales much shorter than strong interaction time scales

Basic review: Jalilian-Marian,Gelis,Iancu,RV: 1002.0333
Textbook: Kovchegov, Levin, Cambridge Univ. Press (2012)

2-D classical EFT

Classical EFT described by QCD Yang-Mills equations in the inifinite momentum frame (P+ $\rightarrow \infty$):

$$D_i \frac{dA^{i,a}}{dy} = g\rho^a(x_t, y)$$

with the solution U = P exp (i$\int_y^{\infty} dy' \frac{\rho(x_{t,}y')}{\nabla_t^2}$)

Color rotation of a probe after interaction with shockwave

A_i =0 | A_i = $-\frac{-1}{ig}$ U∂_i $U^\dagger$

x^-= 0

rapidity variable $y=\ln(x^-/x_0^-)$

Gauge choice A^+= 0
Classical solution: A- = 0

pure gauges (zero field strengths) separated by gluon shockwave discontinuity

$$\langle P|\mathcal{O}|P\rangle \rightarrow \int [d\rho] W_{\Lambda^+}[\rho]\, \mathcal{O}(A_{\rm cl.}[\rho])$$

$$\frac{(2\pi)^3}{2(N_c^2-1)} \frac{dN}{\pi R_A^2 d^2k_\perp}$$

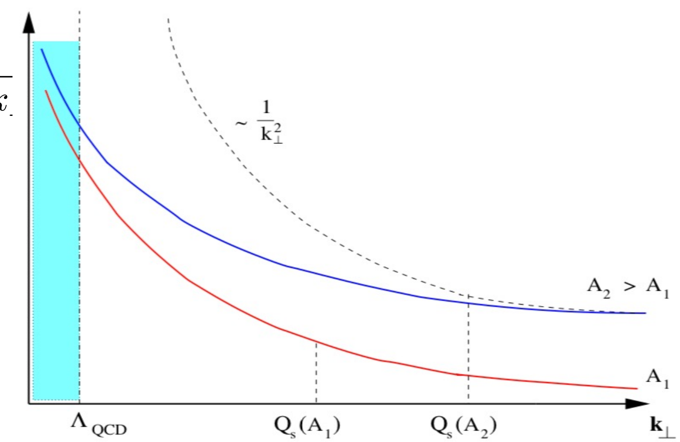

For A >>1 (Gaussian W), compute n-point correlators

Gluon distribution in nucleus:
non-Abelian Weizacker-Williams distribution

Inclusive DIS: dipole evolution

Dipole scattering off the nuclear shock wave

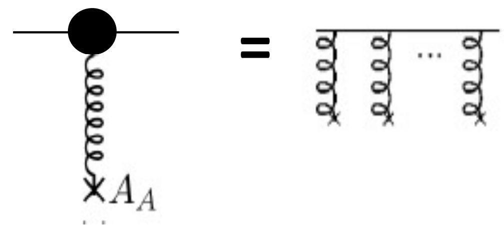

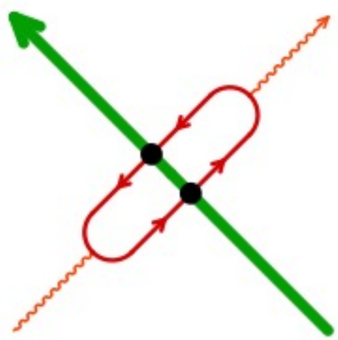

$$\sigma_{\gamma^* T} = \int_0^1 dz \int d^2 r_\perp \, |\psi(z, r_\perp)|^2 \sigma_{\text{dipole}}(x, r_\perp)$$

$$\sigma_{\text{dipole}}(x, r_\perp) = 2 \int d^2 b \int [D\rho] \, W_{\Lambda^+}[\rho] \, T(b + \frac{r_\perp}{2}, b - \frac{r_\perp}{2})$$

$$1 - \frac{1}{N_c} \text{Tr} \left(V \left(b + \frac{r_\perp}{2} \right) V^\dagger \left(b - \frac{r_\perp}{2} \right) \right)$$

$$V = P \, exp(ig \frac{\rho}{\nabla_T{}^2})$$

Inclusive DIS: dipole evolution

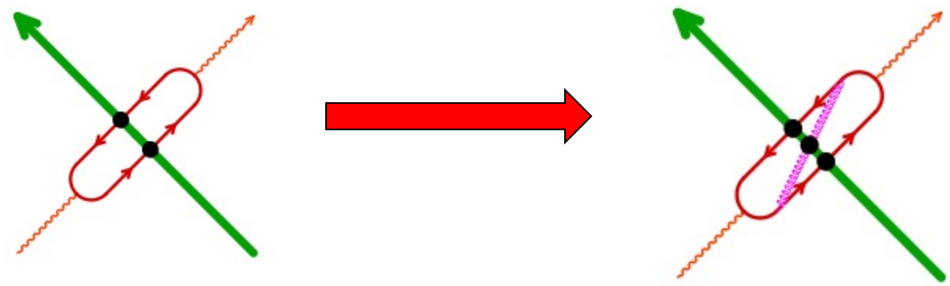

B-JIMWLK eqn. for dipole correlator:

$$\frac{\partial}{\partial Y}\langle \mathrm{Tr}(V_x V_y^\dagger)\rangle_Y = -\frac{\alpha_S N_c}{2\pi^2}\int_{z_\perp} \frac{(x_\perp - y_\perp)^2}{(x_\perp - z_\perp)^2 (z_\perp - y_\perp)^2}\,\langle \mathrm{Tr}(V_x V_y^\dagger) - \frac{1}{N_c}\mathrm{Tr}(V_x V_z^\dagger)\,\mathrm{Tr}(V_z V_y^\dagger)\rangle_Y$$

Dipole factorization:

Y = Ln(1/x)

$$\langle \mathrm{Tr}(V_x V_z^\dagger)\,\mathrm{Tr}(V_z V_y^\dagger)\rangle_Y \longrightarrow \langle \mathrm{Tr}(V_x V_z^\dagger)\rangle_Y \langle \mathrm{Tr}(V_z V_y^\dagger)\rangle_Y$$

A >> 1, $N_c \rightarrow \infty$

Resulting closed form eqn. for a large nucleus is the Balitsky-Kovchegov (BK) equation
- widely used in phenomenological applications

The BFKL equation is the low density $V \approx 1 - ig\rho/\nabla_t^2$ limit of the BK equation…

Dipole evolution in the Color Glass Condensate EFT

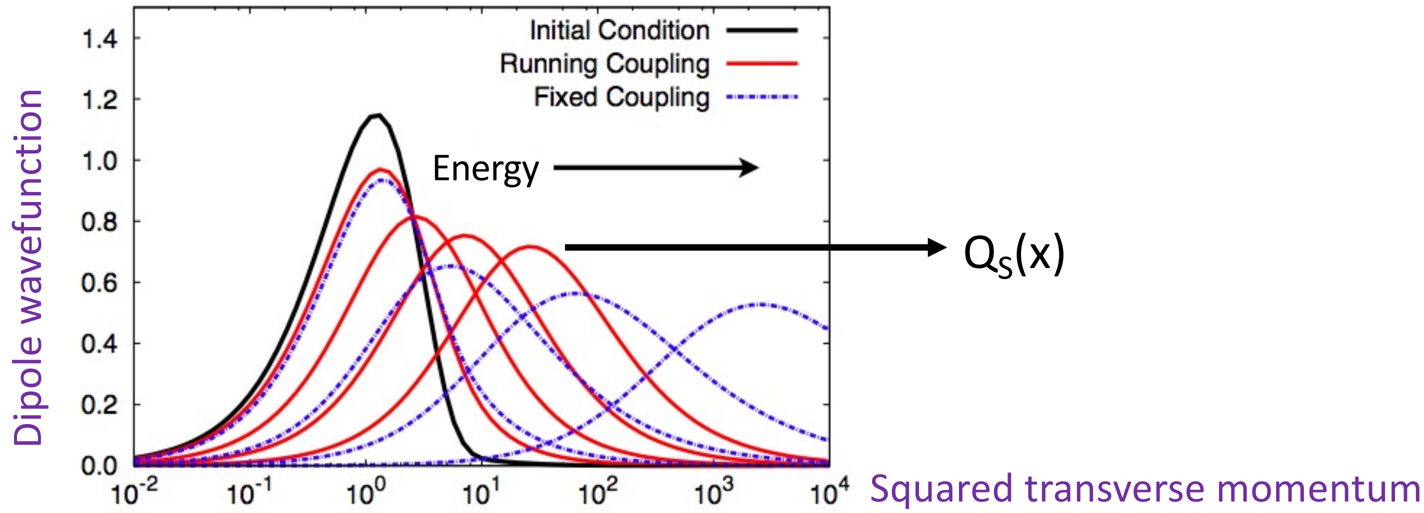

The BK equation describes how $q\bar{q}$ "dipole" probe evolves with energy
– *providing* a *clean demonstration of unitarization in strong fields*

Its dynamics can be mapped* to that of the Fischer-Kolmogorov (FKPP) eqn.
describing the evolution of non-linear wave fronts. Rich synergy with stat. mech.

Munier, Peschanski (2003)

* small caveat

B-JIMWLK hierarchy of many-body correlators in QCD

BFKL: Balitsky-Fadin-Kuraev-Lipatov (1976-1978)
JIMWLK :Jalilian-Marian,Kovner,Leonidov,Weigert (1997);
Iancu,Leonidov,McLerran (2001);
Balitsky (1996)

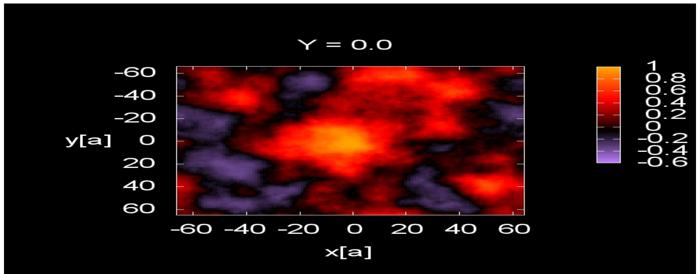

Correlator of Light-like Wilson lines

Dumitru,Jalilian-Marian,Lappi,Schenke,RV, PLB706 (2011)219

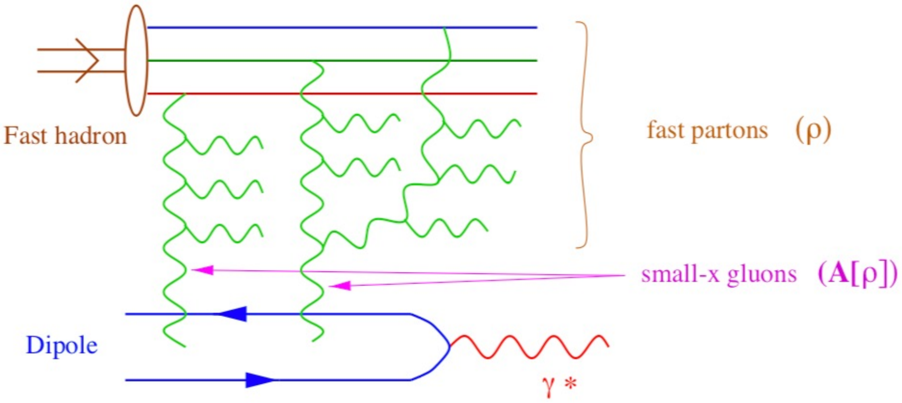

$$\frac{\partial}{\partial Y}\langle \mathcal{O}[\rho]\rangle_Y = \frac{1}{2}\langle \int_{x,y} \frac{\partial}{\partial \rho^a(x)} \chi^{ab}_{x,y} \frac{\partial}{\partial \rho^b(y)} \mathcal{O}[\rho]\rangle_Y$$

"time" "diffusion coefficient"

Diffusion of fuzz of "wee" partons in the functional space of colored fields

Can be represented as a Langevin equation that can be solved numerically
to "leading logs in x" accuracy to compute n-point Wilson line correlators

Framework has a "Lindbladian" interpretation familiar from theory of open quantum systems

Armesto et al., 1901.08080 [hep-ph]

Higher order computations in the CGC (NLO+ NLLx accuracy)

Roy, RV: 1911.04519, 1911:04530

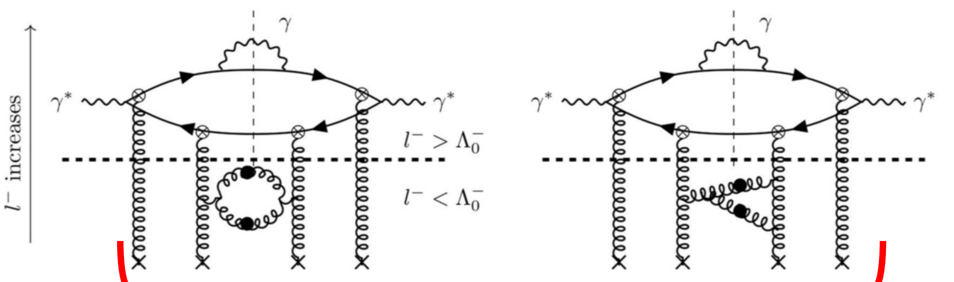

Collect next-to-leading-log (NLLx) pieces $\sim \alpha_S^2 \ln(\Lambda_1^-/\Lambda_0^-)$
+
LO pieces~ α_S^0 in the photon+dijet impact factor

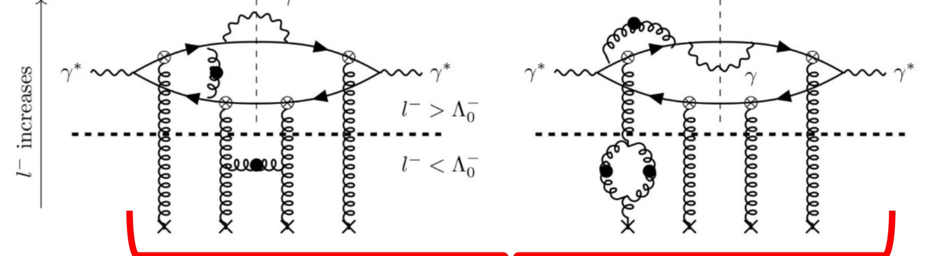

Collect leading log in x (LLx) pieces $\sim \alpha_S \ln(\Lambda_1^-/\Lambda_0^-)$
+
NLO pieces~ α_S in the photon+dijet impact factor

$$\langle \mathrm{d}\sigma^{\mathrm{jet}} \rangle_{\mathrm{NLO+NLL}x} = \int [\mathcal{D}\rho_A] \left\{ W^{NLLx}[\rho_A]\, \mathrm{d}\hat{\sigma}_{\mathrm{LO}}^{\mathrm{jet}}[\rho_A] + W^{LLx}[\rho_A]\, \mathrm{d}\hat{\sigma}_{\mathrm{NLO}}^{\mathrm{jet;finite}}[\rho_A] \right\}$$

$$\simeq \int [\mathcal{D}\rho_A] \left(W^{NLLx}[\rho_A] \left\{ \mathrm{d}\hat{\sigma}_{\mathrm{LO}}^{\mathrm{jet}}[\rho_A] + \boxed{\mathrm{d}\hat{\sigma}_{\mathrm{NLO}}^{\mathrm{jet;finite}}[\rho_A]} \right\} + O(\alpha_S^3 \ln(\Lambda_1^-/\Lambda_0^-)) \right)$$

$$W_{\Lambda_0^-}^{NLLx}[\rho_A] = \left\{ 1 + \ln(\Lambda_1^-/\Lambda_0^-)(\mathcal{H}_{LO} + \mathcal{H}_{NLO}) \right\}$$

NLO impact factor

Accuracy of result

NLO evolution equations

NLO BFKL: Fadin, Lipatov (1998)
NLO JIMWLK: Balitsky, Chirilli, arXiv:1309.7644, Grabovsky, arXiv:1307.5414; Caron-Huot, arXiv:1309.6521, Kovner,Lublinsky,Mulian, arXiv:1310.0378, Lublinsky, Mulian, arXiv:1610.03453
NNLO BK for SYM: Caron-Huot and Herranen, arXIv:1604.07417

Some work in progress in theory and phenomenology

NLO Impact factor in DIS

- Structure functions (fully inclusive DIS)

  Balistky-Chirilli (2012)
  Beuf (2017)
  Hänninen, Lappi, Paatelainen (2017)
  Beuf, Hänninen, Lappi, Mäntysaari (2020)

- Exclusive dijet

  Boussarie, Grabovsky, Szymanowski, Wallon (2016,2019)

- Exclusive J/ψ

  Mäntysaari, Penttala (2021)

- Inclusive photon+dijet

  Roy, Venugopalan (2019)

- Inclusive back-to-back dijets within TMD

  Mueller, Xiao, Yuan (2013)
  Xiao, Yian, Zhou (2017)

NLO computations in parallel of final states in p+A collisions at RHIC+LHC

Di-jet production in e+A collisions

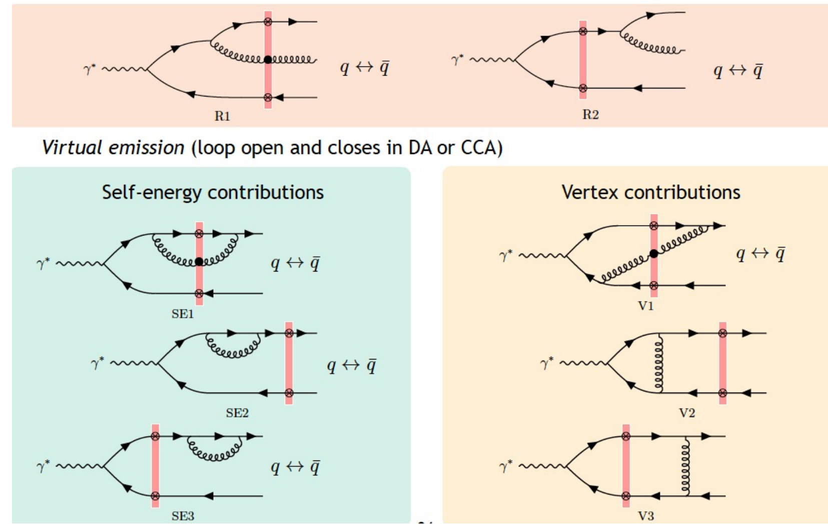

Caucal, Salazar, RV, arXiv:2108.06347

Key element in our approach are shock wave quark and gluon propagators in momentum space

McLerran,RV (1994,1998); Balitsky, Belitsky (2001)

Identical to Lipatov's quark-quark-reggeon and gluon-gluon-reggeon propagators

Hentschinski, arXiv:1802.06755

Color Memory and gravitational memory

Ball,Pate,Raclariu,Strominger,RV,
Annals of Physics 407 (2019) 15

$x^{\pm} = \frac{t \pm z}{\sqrt{2}}$

$A_i = 0$ $\quad$ $A_i = -\frac{-1}{ig} U \partial_i U^{\dagger}$

$x^{-} = 0$

In QCD's Regge limit, gluon "shockwave" represents two "pure gauge" color field vacua separated by a light-cone discontinuity

$y = \mathrm{Log}(x^-/x_0^-)$

Solution: $U = P \exp \left(i \int_y^{\infty} dy' \, \frac{\rho(x_t, y')}{\nabla_t^2} \right)$

U represents the *color memory* of a color rotation and $p_T \sim Q_S$ kick retained by a quark-antiquark pair long after passage of the gluon shockwave

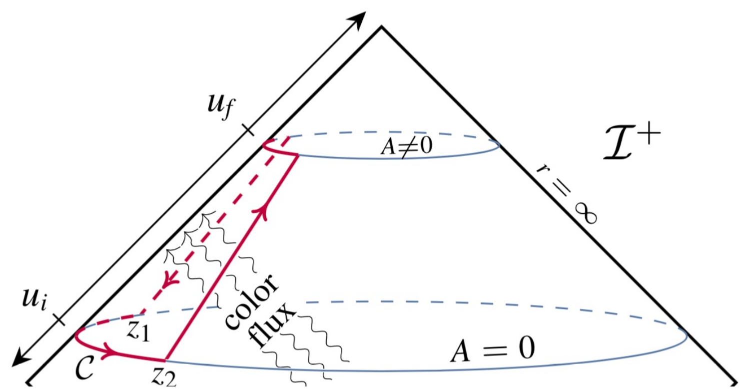

It is the Yang-Mills equivalent of the gravitational memory effect

Pate, Raclariu, Strominger, PRL (2017)

Infrared memory and asymptotic symmetries

Strominger,arXiv:1703.05448

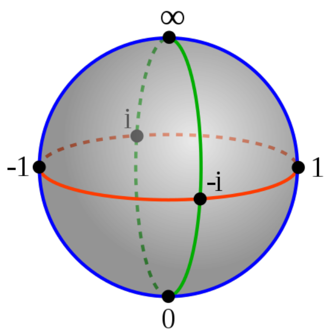

Riemann/Celestial sphere: stereographic projection of 2-D transverse plane

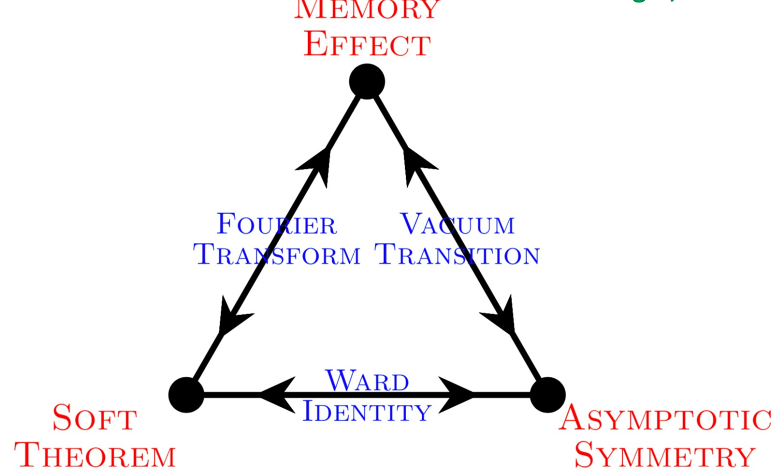

Gravitational memory related to infinite dimensional Bondi-Metzner-Sachs (BMS) symmetry of gravity at null infinity (fixed retarded time and r→ ∞) and to Weinberg’s soft graviton theorem

Similar realization for QED provides a deep understanding of Low’s soft photon theorem and structure of collinear/soft divergences of scattering amplitudes (a la Fadeev-Kulish, 1970)

Infrared Memory: from EIC to LISA, etc…

JLEIC

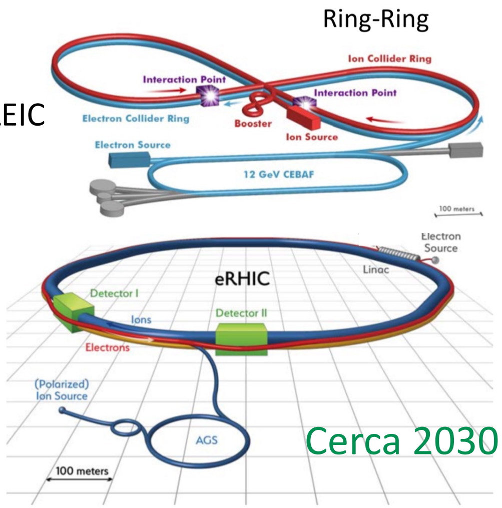

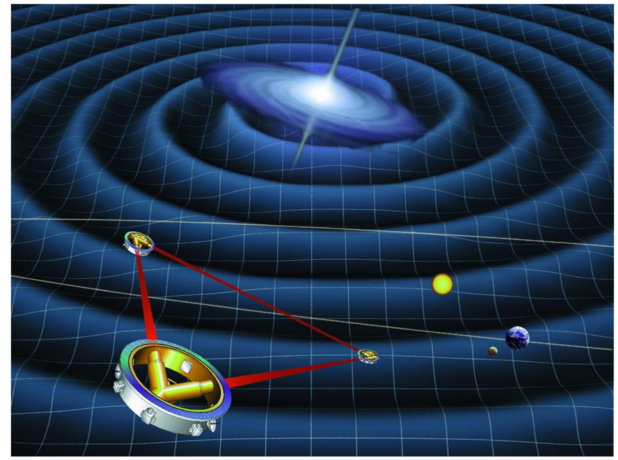

Cerca 2030s ?

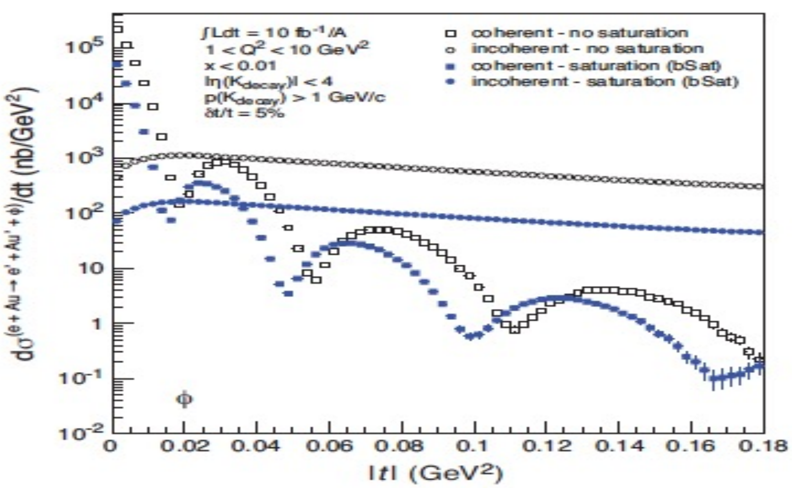

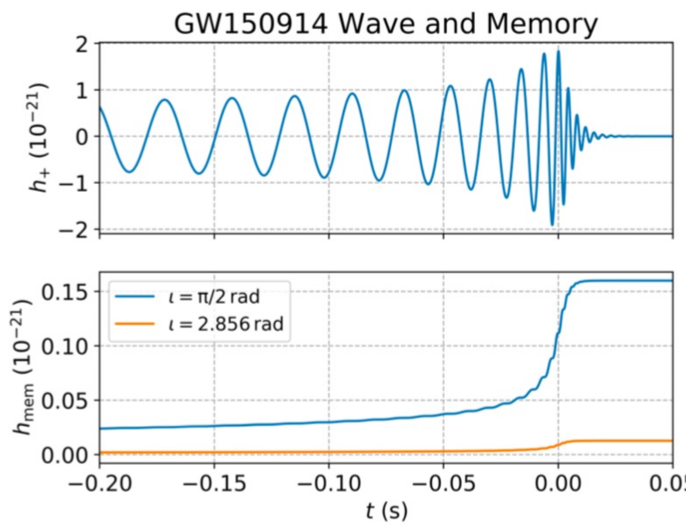

QCD and gravity: The CGC-Black Hole correspondence

Dvali, RV, arXiv:2106.11989

$2 \to N + 2$ amplitudes in the Regge limit of gravity: the Lipatov-ACV approach and the double copy

HIGH-ENERGY SCATTERING IN QCD AND IN QUANTUM GRAVITY AND TWO-DIMENSIONAL FIELD THEORIES

L.N. LIPATOV*

We construct effective actions describing high-energy processes in QCD and in quantum gravity with intermediate particles (gluons and gravitons) having the multi-Regge kinematics. The S-matrix for these effective scalar field models contains the results of the leading logarithmic approximation and is unitary. It can be expressed in terms of correlation functions for two field theories acting in longitudinal and transverse two-dimensional subspaces.

NPB 364 (1991) 614; 157 cites in INSPIRE

Effective action and all-order gravitational eikonal at planckian energies

AMATI,CIAFALONI,VENEZIANO **NPB403 (1993)707**

Building on previous work by us and by Lipatov, we present an effective action approach to the resummation of all semiclassical (i.e. $O(\hbar^{-1})$) contributions to the scattering phase arising in high-energy gravitational collisions. By using an infrared-safe expression for Lipatov's effective action, we derive an eikonal form of the scattering matrix and check that the superstring amplitude result is reproduced at first order in the expansion parameter R^2/b^2, where R, b are the gravitational radius and the impact parameter, respectively. If rescattering of produced gravitons is neglected, the longitudinal coordinate dependence can be explicitly factored out and exhibits the characteristics of a shock-wave metric while the transverse dynamics is described by a reduced two-dimensional effective action. Singular behaviours in the latter, signalling black hole formation, can be looked for.

The World as a Hologram

LEONARD SUSSKIND

Wee partons, by contrast, are not subject to Lorentz contraction. This implies that in the Feynman Bjorken model, the halo of wee partons eternally "floats" above the horizon at a distance of order $10^{-13}cm$ as it transversley spreads. The remaining valence partons carry the various currents which contract onto the horizon as in the Einstein Lorentz case.

By contrast, both the holographic theory and string theory require all partons to be wee. No Lorentz contraction takes place and the entire structure of the string floats on the stretched horizon. I have explained in previous articles how this behavior prevents the accumulation of arbitrarily large quantities of information near the horizon of a black hole. Thus we are led full circle back to Bekenstein's principle that black holes bound the entropy of a region of space to be proportional to its area.

J.Math.Phys. **36 (1995) 6377; 3048 cites**

In Acknowledgements:

Finally I benefitted from discussions with Kenneth Wilson and Robert Perry, about boosts and renormalization fixed points in light front quantum mechanics and Lev Lipatov about high energy scattering.

These works do not explicitly discuss parton saturation which leads to a perspective I will discuss shortly

Classicalization and unitarization in Gravity: The Black Hole N Portrait

Dvali, Gomez, arXiv:1112.3359
Dvali,Guidice,Gomez,Kehagis, arXiv:1010.1415

Black Holes as macroscopic quantum states

When $N = \frac{1}{\alpha_{gr}}$, the dense graviton state unitarized by forming a Black Hole

The Black Hole N Portrait suggests gravity is UV self-complete due classicalization at a weak coupling scale

Gravitons have wavelengths $\lambda = R_S = \sqrt{N}\, L_P$

$$\alpha_{gr} = \frac{L_P^2}{\lambda^2} = \frac{1}{N} \xrightarrow{N\to\infty} 0$$

$R_S = 2GM$ Schwarzchild radius
$L_P = \sqrt{\hbar G}$ Planck Length
$M_P = \sqrt{\hbar/G}$ Planck Mass

Black Hole evaporation Rate

$$\Gamma = 6\, n_h (1+N) \sim \cancel{\alpha_{gr}^2} R_S^2 \frac{\cancel{N^2}}{R_S^3} \equiv \frac{1}{R_S}$$

For $T_H = \frac{\hbar}{R_S} = \frac{\hbar}{\sqrt{N}\, L_P}$

obtain familiar expressions

$$\frac{dM}{dt} = -\frac{T^2}{\hbar}$$

and half-life

$$\tau_{BH} = \frac{\hbar^2}{T^3 G} \equiv N^{3/2} L_P$$

Classicalization and unitarization in Gravity: The Black Hole N Portrait

Bekenstein-Hawking bound

(for a nice discussion, see Bousso, arxlv:1810.01880)

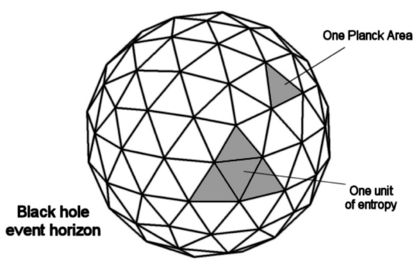

The Bekenstein entropy bound is given by $S \leq 2\pi E R/\hbar$

In the Black Hole N portrait, this is given by $S \leq 2\pi\, N\, Q_S\, R_S$

which is saturated when $N = \frac{1}{\alpha_{gr}} \rightarrow S_{Bek} = \frac{1}{\alpha_{gr}}$

Here E = N Q_S is the energy in a critically packed volume = R_S^3 of quanta, and $Q_S = 1/R_S$

$$S_{Bek} = \frac{1}{\alpha_{gr}} = \frac{R_S^2}{L_P^2} = \frac{Area}{4G} = S_{BH}$$

The entropy can also be expressed in terms of a Goldstone decay constant corresponding to spontaneous breaking of Poincare invariance by the graviton condensate: $f^2 = N\, QS^2$

Dvali, arXiv:0907.07332

The entropy in these units is $S_{BH} = Area \times f^2$

At the critical point $N = \frac{1}{\alpha_{gr}}$, the saturation of the BH bound also leads to unitarization !

$$\sigma^{BHNP}_{2\to N} = N!\, \alpha_{gr}^N\, e^{S_{BH}} \simeq \cancel{N^N} e^{-N} \left(\cancel{\frac{1}{N}}\right)^N e^{\frac{1}{\alpha_{gr}}} = e^{-\frac{1}{\alpha_{gr}} + \frac{1}{\alpha_{gr}}} \sim O(1)$$

Dvali,Gomez,Isermann,Lust,Stieberger arXiv:1409.7405

Away from the critical point, the cross-section for BH formation drops exponentially !

The CGC/BHNP correspondence: Bekenstein entropy

Dvali, RV, 2106.11989

We can use this direct correspondence to conjecture the maximal Bekenstein entropy of the CGC

Since the typical momenta of saturated wee gluons is Q_S , the CGC energy is N Q_S in a "color domain" of radius Q_S^{-1} - and the entropy argument goes through as previously:

$$S_{\mathrm{CGC}} = \frac{1}{\alpha_S}$$

Further, one can have 1/ α_S wee partons in a rapidity interval Y, this gives $\frac{dS_{CGC}}{dY} = \text{constant}$

$$S_{proton} = \mathrm{n_D}\, S_{\mathrm{CGC}}$$

Inside a confining radius of Λ_{QCD}^{-1}, of the Lorentz contracted proton at high energies, there can be $\frac{Q_S^2}{\Lambda_{QCD}^2}$ = n_D domains

Several discussions in the literature:
Our result is in agreement with Kharzeev, Levin, arXiv:1702.03489

The CGC/BHNP correspondence

Dvali, RV, 2106.11989

From the previous discussion, we begin to glimpse the elements of the CGC/BHNP correspondence with a region of space $R_S = Q_S^{-1}$ of the CGC mapped on to a Black Hole on analogous radius determined by the saturation of the graviton condensate:

The scale at which this occurs is a weak coupling scale in both theories:

$$\text{for BHNP}: \quad Q_S^{-1} = \sqrt{N} M_P^{-1} \, ;$$
$$\text{for CGC}: \quad Q_S = \sqrt{N} \Lambda_{\text{QCD}}$$

One can equivalently express this correspondence in terms of a Goldstone decay scale $f^2 = N\, Q_S^2$ corresponding to broken Poincare invariance in both theories; in the CGC, this scale is set by the onset of gluon screening. The area law for the entropy is identical in both theories in terms of this scale

The direct correspondence between the two theories only occurs at $Q=Q_S$ where the physics is universal - It is independent of the details of the dynamics of the wee partons

The existence of a double copy between the two theories is however suggestive that it can be extended to a “classical” double copy between the gluon and graviton classical shockwaves

Review on classical double copy: C. White, arXiv:1708.07056

Spacetime evolution of a heavy-ion collision

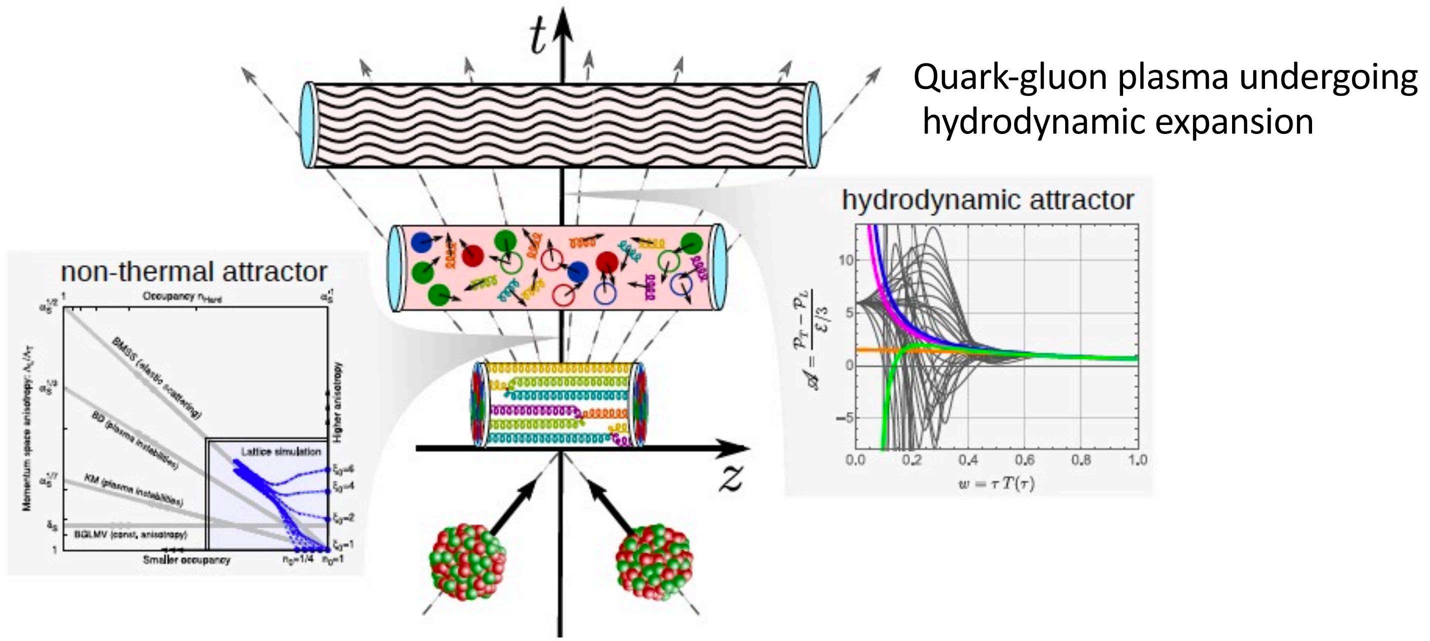

QCD thermalization: Ab initio approaches and interdisciplinary connections

Jürgen Berges, Michal P. Heller, Aleksas Mazeliauskas, and Raju Venugopalan

Rev. Mod. Phys. **93**, 035003 (arXiv:2005.12299)

The Chiral Magnetic Effect

Kharzeev,McLerran,Warringa (2007)
Fukushima,Kharzeev,Warringa (2008)

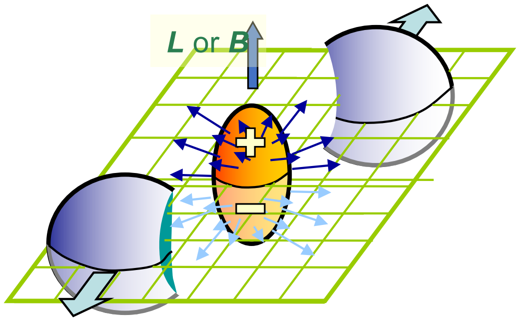

External (QED) magnetic field
- As strong as 10^{18} Gauss !

+

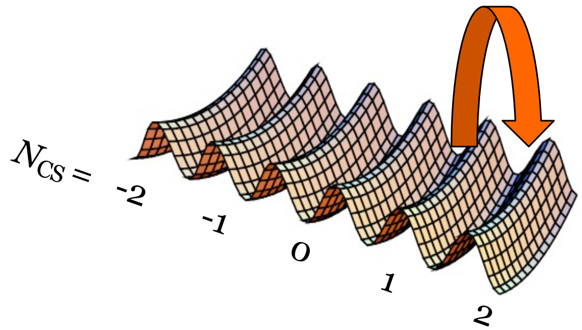

Over the barrier topological (sphaleron) transitions … analogous to proposed mechanism for Electroweak Baryogenesis

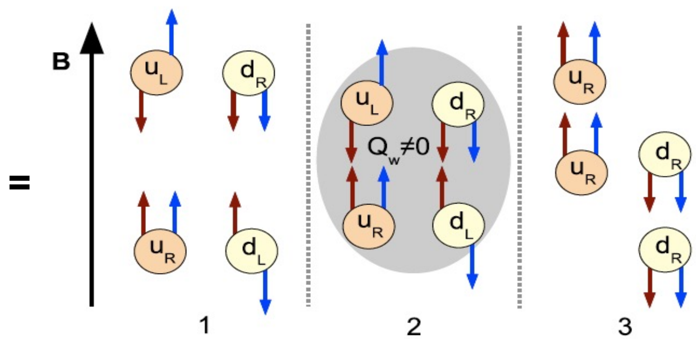

$$\vec{J}_{\rm CME} = \frac{e^2}{2\pi^2}\,\mu_5\,\vec{B}$$

Chiral magnetic effect

Topology in heavy-ion collisions:The Chiral Magnetic Effect

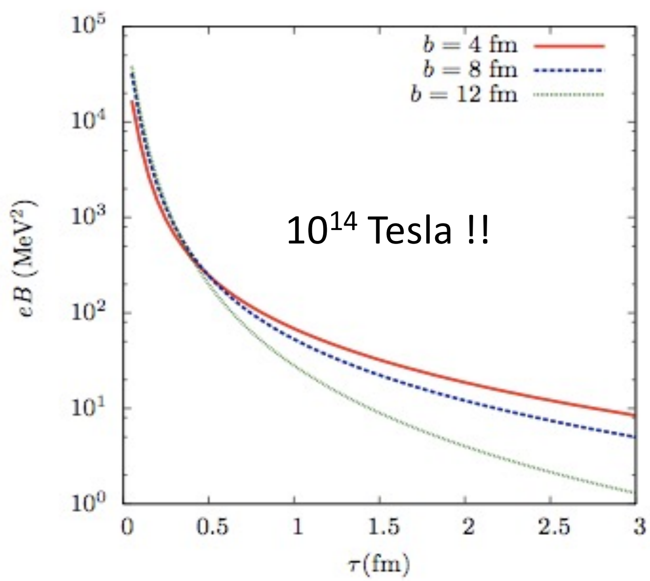

External B field dies rapidly…
Effect most significant,
for transitions at early times

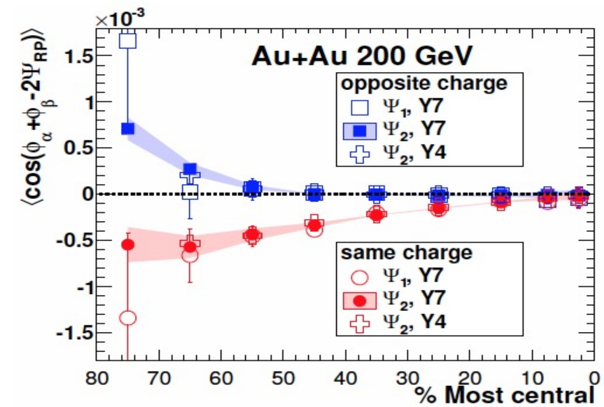

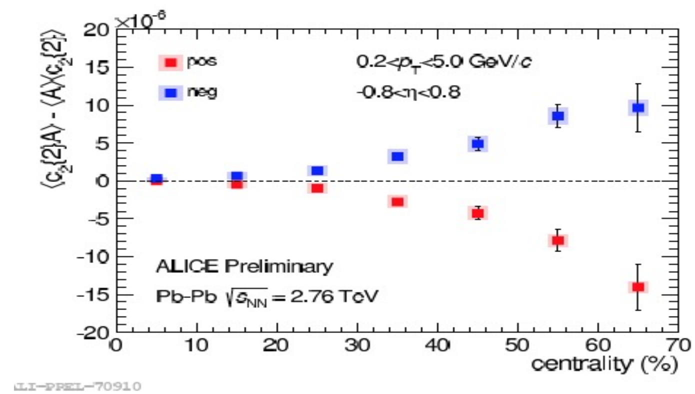

Ruled out definitively in isobar RHIC collisions at the highest energy. Prospects may still exist at lower energies

STAR, arXiv:2109.00131

Sphaleron transitions in QCD

Sphaleron: spatially localized, unstable finite energy classical solutions (σφαλερος -``ready to fall”)

EW theory: Klinkhamer, Manton, PRD30 (1984) 2212
QCD: McLerran,Shaposhnikov,Turok,Voloshin, PLB256 (1991) 451

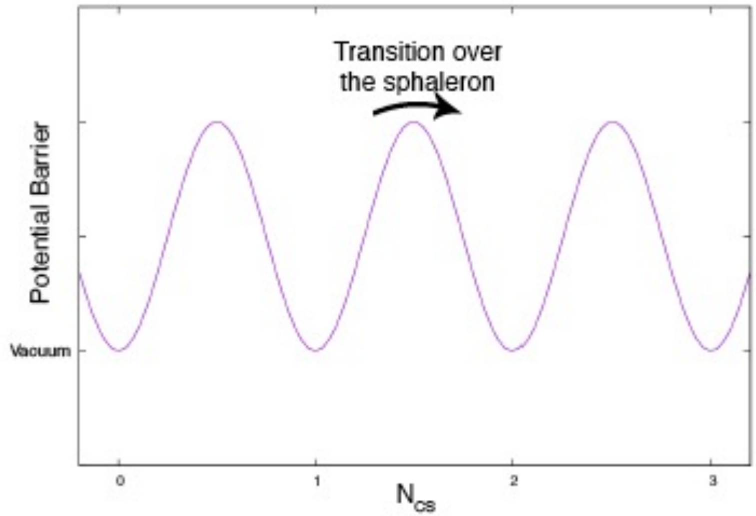

Chiral Anomaly:

$$\partial_\mu J^\mu_{5,f} = 2m_f \bar{q}\gamma_5 q - \frac{g^2}{16\pi^2} F^a_{\mu\nu}\tilde{F}^{\mu\nu,a} \quad = \partial_\mu K^\mu \text{ for } m_f=0$$

Chern-Simons current:

$$K^\mu = \frac{g^2}{32\pi^2}\epsilon^{\mu\nu\rho\sigma}\left(F^a_{\nu\rho}A^a_\sigma - \frac{g}{3} f_{abc}A^b_\nu A^c_\rho A^c_\sigma\right)$$

Chern-Simons #:

$$N_{CS}(t) = \int d^3x\, K^0(t,\mathbf{x})$$

Rate of change of CS #

$$\frac{dN_{CS}(t)}{dt} = \frac{g^2}{8\pi^2}\int d^3x\, E^a_i(\mathbf{x})B^a_i(\mathbf{x})$$

Key quantity: Sphaleron transition rate

$$\Gamma^{eq} = \lim_{\delta t -> \infty} \frac{\langle (N_{\rm CS}(t+\delta t) - N_{\rm CS}(t))^2\rangle_{\rm eq}}{V\delta t}$$

Thermal sphaleron transition rate

Mace,Schlichting,RV (2016)

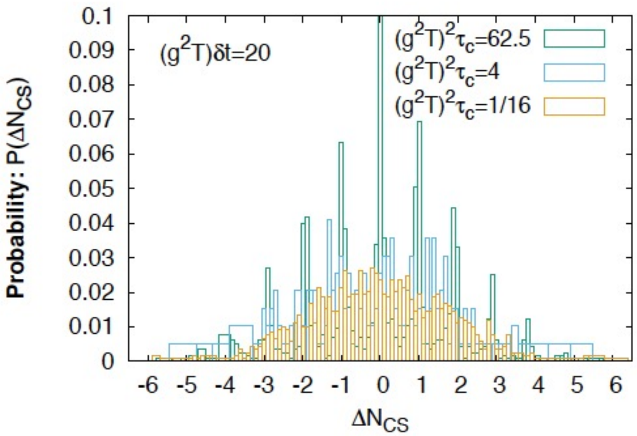

Cooled configurations—with UV modes systematically removed - contain increasingly soft infrared modes that cluster about integer values of CS #

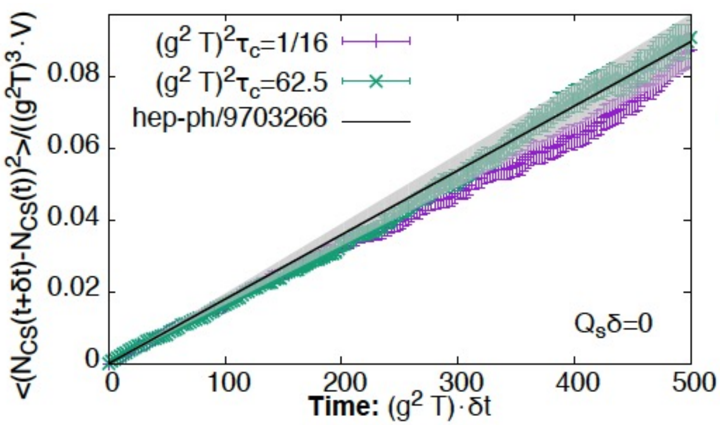

Moore, Tassler, arXiv:1011.1167

$$\Gamma_{\rm sphal} = (132 \pm 4) \left(\frac{g^2 T^2}{m_{\rm D}^2}\right) \left(\ln\frac{m_{\rm D}}{\gamma} + 3.0410\right) \alpha_{\rm s}^5 T^4 \,,$$

$$\gamma = \frac{N_{\rm c} g^2 T}{4\pi} \left(\ln \frac{m_{\rm D}}{\gamma} + 3.041\right) \,,$$

$$m_{\rm D}^2 = \frac{2N_{\rm c} + N_{\rm f}}{6} g^2 T^2 = \frac{6 + N_{\rm f}}{6} g^2 T^2 \,.$$

Parametric form predicted by Arnold, Son, Yaffe

Sphaleron transitions in the Glasma

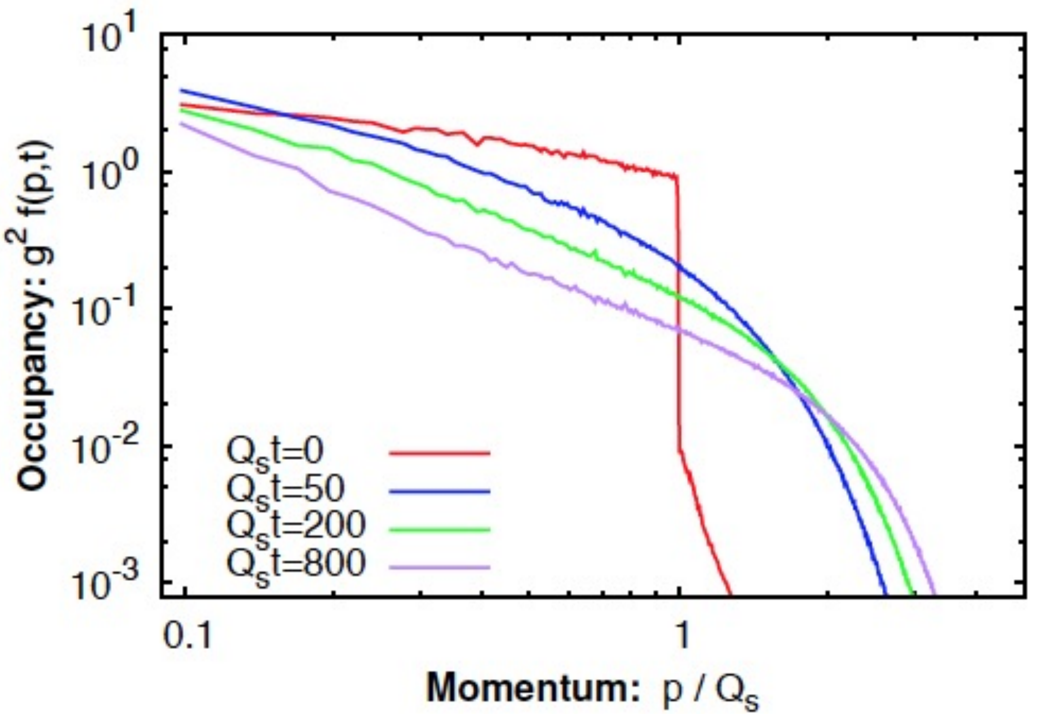

For simplicity, only consider Glasma in a box, and SU(2) gauge theory

Mace,Schlichting,RV (2016)

Emergence of infrared structure in the Glasma

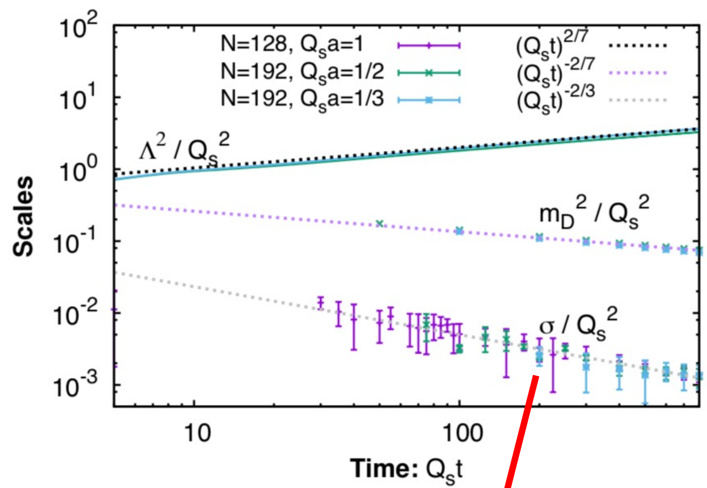

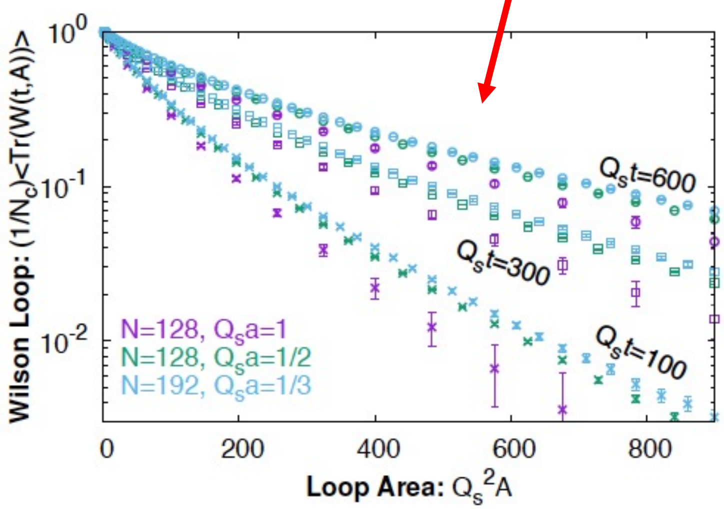

A (parametrically) one scale Glasma evolves towards the separation of length scales characteristic of a QGP:

$T >> gT >> g^2T$

Trace of spatial Wilson loop obeys area law – string tension σ sensitive to infrared dynamics at the magnetic scale

Topological transitions in the Glasma

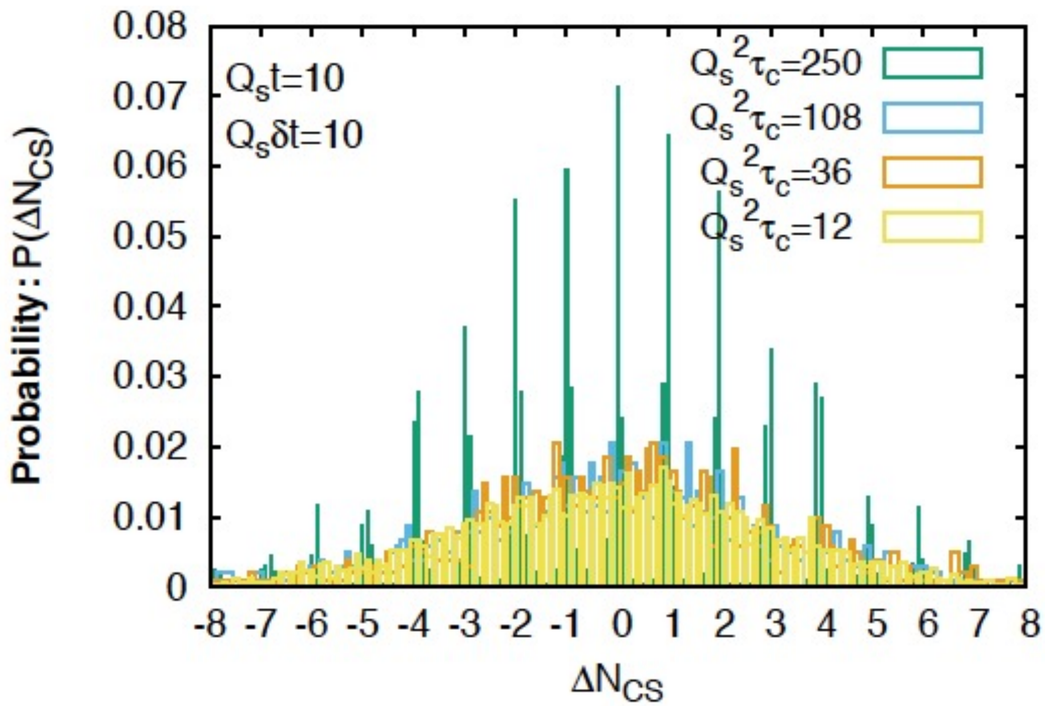

First evidence that "cooled" soft glue configurations in the Glasma are topological!

Mace,Schlichting,Venugopalan, PRD (2016)

Topological transitions in the Glasma

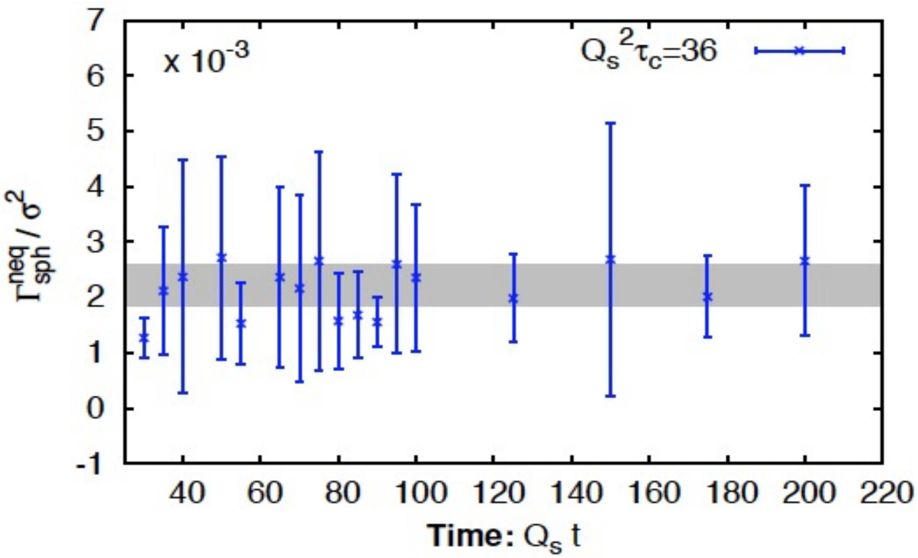

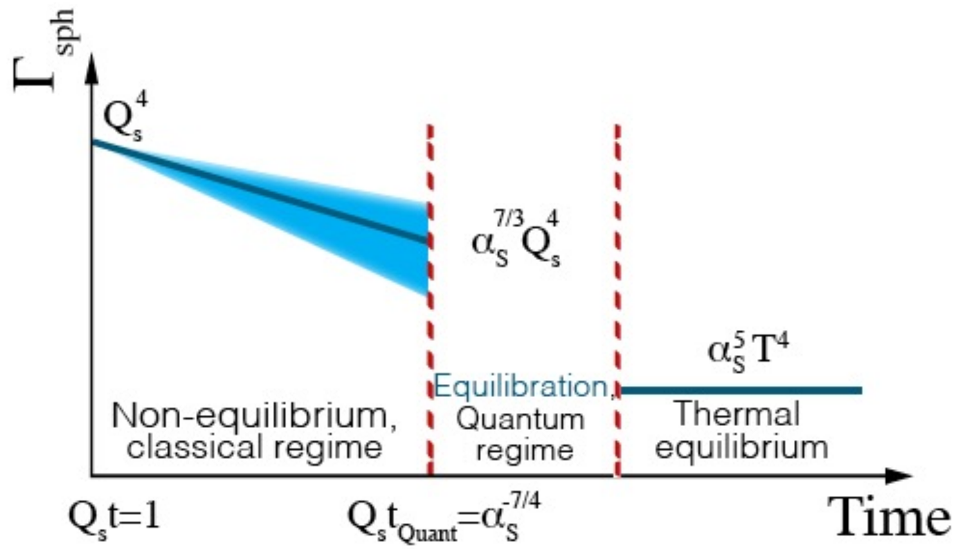

Sphaleron transition rate scales with the string tension in the Glasma- rate is large at early times !

Mace,Schlichting,Venugopalan,PRD (2016)

An effective theory of Wilson loops could capture the nonequilibrium dynamics of the Glasma ?

The proton’s spin puzzle: new tools for an old problem

The proton's spin puzzle: a many-body picture

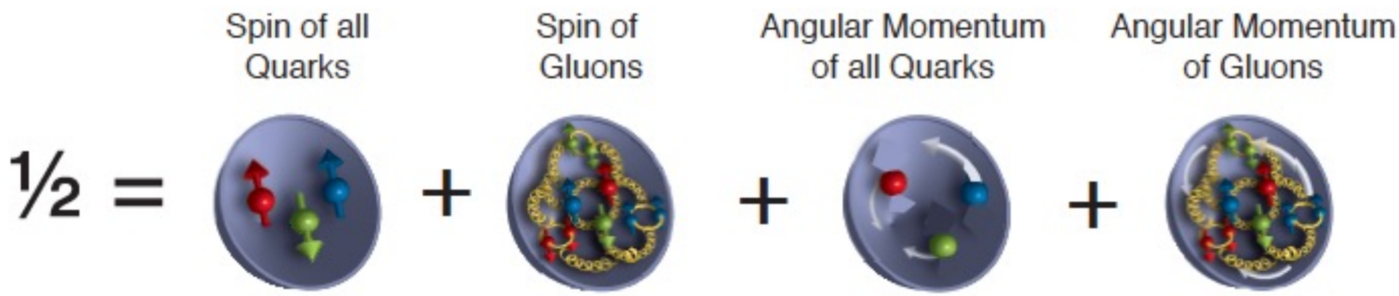

Fixed target DIS experiments showed that quarks carry only about 30% of the proton's spin

"Spin crisis": failure of the quark model ("Ellis-Jaffe sum rule") picture of relativistic "constituent" quarks
-quark helicity ($\Delta\Sigma$) much smaller than quark model expectations

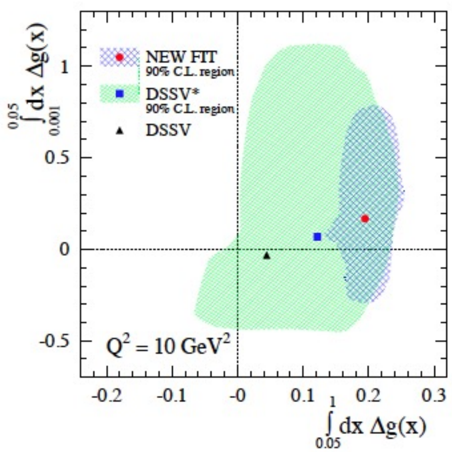

Evidence for gluon spin (ΔG) from RHIC
but large uncertainties from small x

D. De Florian, R. Sassot, M. Stratmann, W. Vogelsang, PRL 113 (2014)

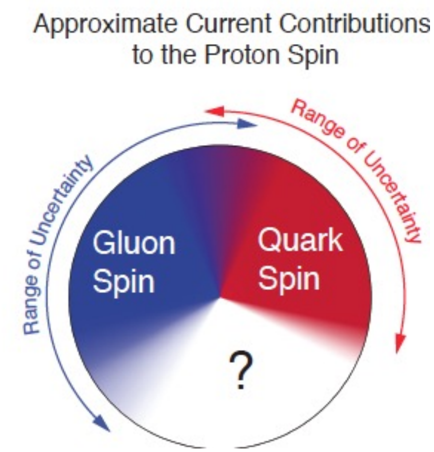

Resolving the proton's spin puzzle: the g_1 structure function

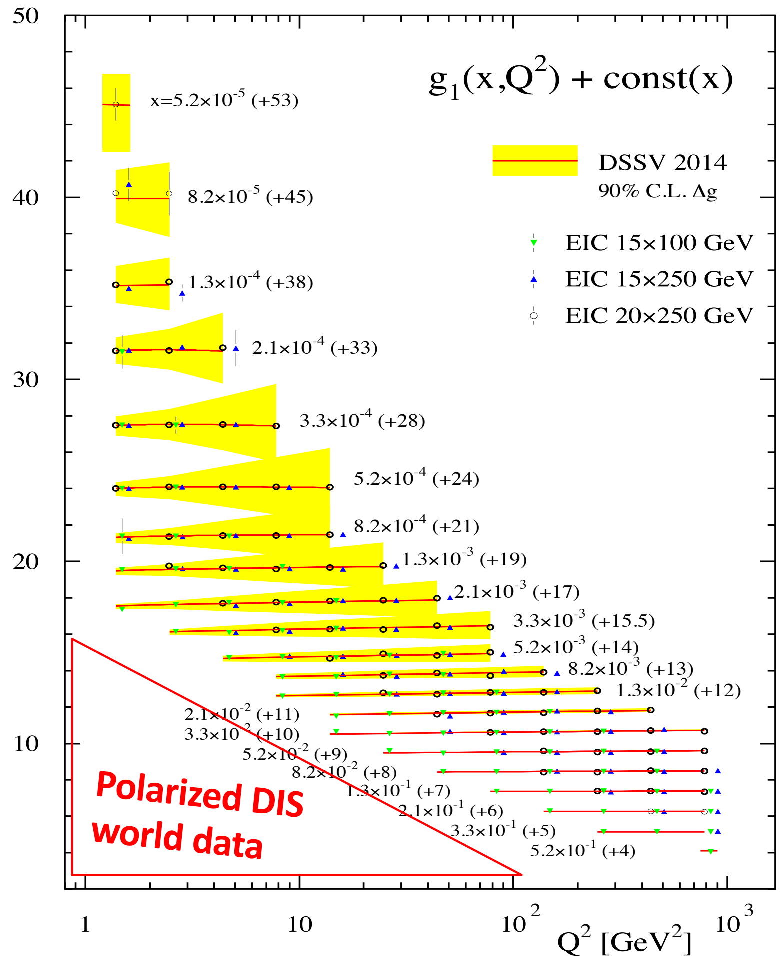

g_1 extracted from longitudinal spin asymmetry

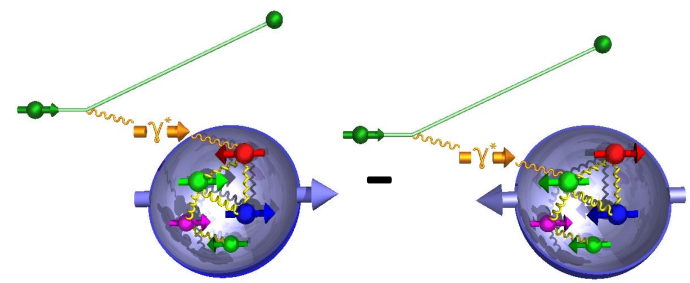

$$\Delta\Sigma(Q^2) \propto \int_0^1 dx\, g_1(x,Q^2) \rightarrow \text{quark contribution}$$

$$\frac{dg_1}{d\log(Q^2)} \overset{?}{\sim} -\Delta g(x,Q^2) \rightarrow \textbf{gluon contr.}$$

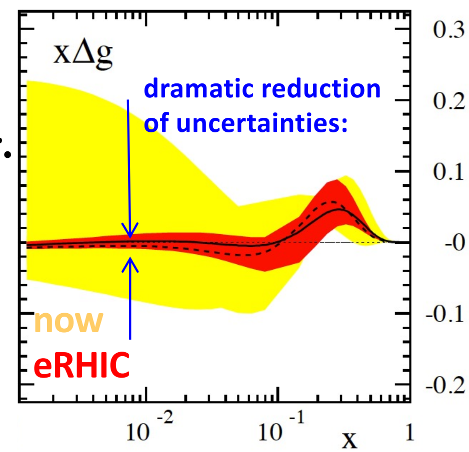

Resolving the proton's spin puzzle: the g_1 structure function

Aschenauer et al., Rep. Prog. Phys. 82, 024301 (2019)

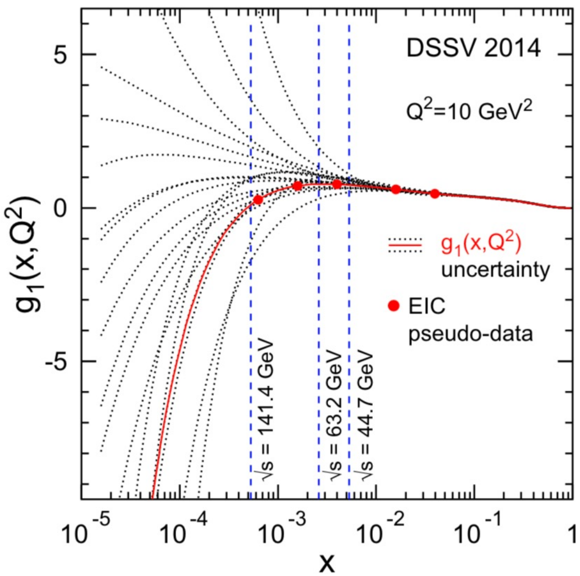

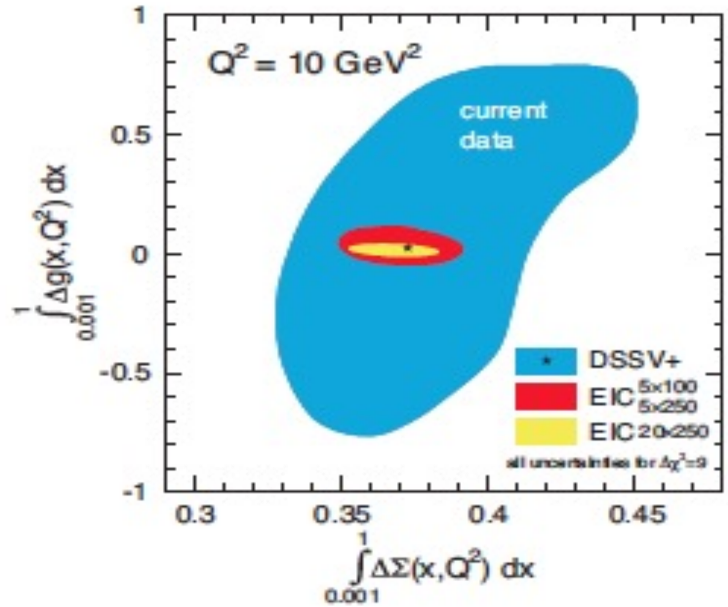

In the parton model, at leading twist

$$g_1(x_B, Q^2) = \frac{1}{2}\sum_f e_f^2 \left(\Delta q_f(x_B, Q^2) + \Delta\bar{q}_f(x_B, Q^2)\right)$$

$$\Delta q(x) =$$

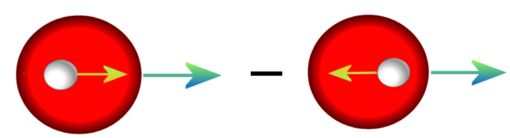

Most generally, $g_1(x, Q^2) = \frac{1}{8\lambda}\epsilon_T^{\mu\nu}\tilde{W}_{\mu\nu}(q, P, S)$

where $\widetilde{W}^{\mu\nu}$ is the antisymmetric part of $W^{\mu\nu}$

$S^\mu = \frac{2\lambda}{m_P} P^\mu$ and $\lambda = \pm 1/2$

Isosinglet axial vector current and the chiral anomaly

$$\int_0^1 g_1(x,Q^2) = \frac{1}{18}\left(3F + D + 2\,\Sigma(Q^2)\right)$$

$$S^\mu\,\Delta\Sigma \;=\; \langle P,S\,|\,\bar{\psi}\,\gamma^\mu\gamma_5\,\psi\,|\,P,S\rangle \;\equiv\; \langle P,S\,|\,j_5^\mu\,|\,P,S\rangle$$

J_5^μ is the isosinglet axial vector current

$U_A(1)$ violation from the chiral anomaly:

$$\boxed{\partial_\mu J_5^\mu = 2n_f\partial_\mu K^\mu + \sum_{i=1}^{n_f} 2im_i\bar{q}_i\gamma_5 q_i}$$

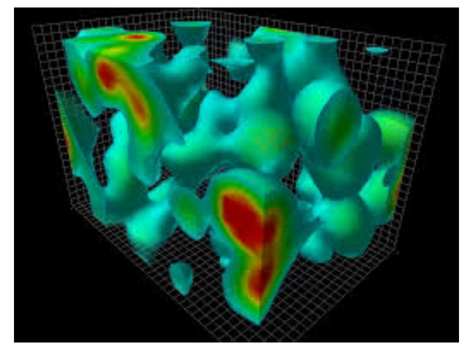

Divergence of C-S current $\propto$ topological charge density

where the Chern-Simons current $K_\mu = \frac{g^2}{32\pi^2}\epsilon_{\mu\nu\rho\sigma}\left[A_a^\nu\left(\partial^\rho A_a^\sigma - \frac{1}{3}gf_{abc}A_b^\rho A_c^\sigma\right)\right]$

The Adler-Bell-Jackiw chiral (triangle) anomaly

$$\langle P', S | J_5^\kappa | P, S\rangle = \int d^4y \frac{\partial}{\partial A_{5\kappa}(y)} \Gamma[A, A_5]\Big|_{A_5=0} e^{ily} \equiv \Gamma_5^\kappa[l]$$

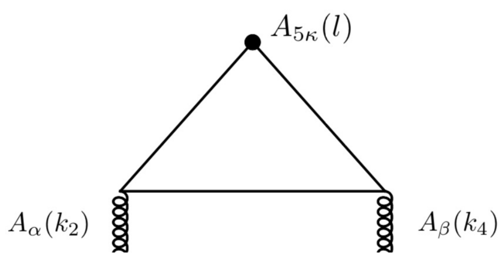

$$= \frac{1}{4\pi^2} \frac{l^\kappa}{l^2} \int \frac{d^4k_2}{(2\pi)^4} \int \frac{d^4k_4}{(2\pi)^4} \, \mathrm{Tr}_c F_{\alpha\beta}(k_2) \tilde{F}^{\alpha\beta}(k_4) \; (2\pi)^4 \delta^4(l + k_2 + k_4)$$

Famous infrared pole of anomaly. One loop exact: Adler-Bardeen theorem

Key insight from Fujikawa:

Anomaly arises from the non-invariance of the path integral measure under chiral (γ_5) rotations

$$e^{iW} = \int \underbrace{\mathcal{D}A\mathcal{D}\bar{q}\mathcal{D}q}_{} \; \exp\left[i \int dx (\mathcal{L}_{\mathrm{QCD}} + V_5^{\mu a} J_{\mu 5}^a + V^{\mu a} J_\mu^a + \theta Q + S_5^a \phi_5^a + S^a \phi^a) \right]$$

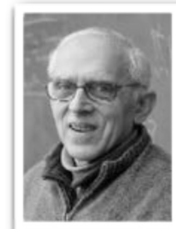

Steven Adler

John S. Bell

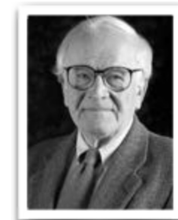

Roman Jackiw

William A. Bardeen

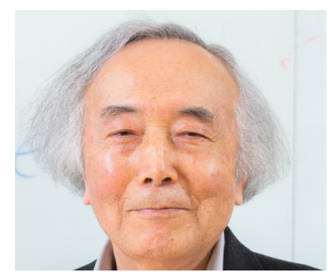

Kazuo Fujikawa

Anomalies in the worldline formulation of QFT

Fermion action in background of scalar, pseudoscalar, vector and axial vector fields:

$$S_{\mathrm{fermion}}[\bar{\Psi}, \Phi, \Pi, A, B, \Psi] = \int d^4x\, \bar{\Psi}^I \left[i\partial\!\!\!/ - \Phi + i\gamma^5 \Pi + A\!\!\!/ + \gamma^5 B\!\!\!/ \right]^{IJ} \Psi^J$$

Effective action: $-\mathcal{W}[A, B, \Phi, \Pi] = \mathrm{Ln}\,\mathrm{Det}\,[\mathcal{D}]$ with $\mathcal{D} = p\!\!\!/ - i\Phi(x) - \gamma_5\,\Pi - A\!\!\!/ - \gamma_5 B\!\!\!/$

Split into real and imaginary parts: $\mathcal{W}_R = -\frac{1}{2}\mathrm{Ln}\left(\mathcal{D}^\dagger \mathcal{D}\right)$; $\mathcal{W}_I = \frac{1}{2}\mathrm{Arg}\,\mathrm{Det}\left(\mathcal{D}^2\right)$

Entire dynamics of the anomaly comes from W_I - the phase of the Dirac determinant

Remarkable observation:
W_I can be expressed as a worldline Lagrangian of 0+1- bosonic (coordinate) and Grassmann fields

D'Hoker, Gagne, hep-th/9508131

The box diagram for polarized DIS ($g_1(x,Q^2)$)

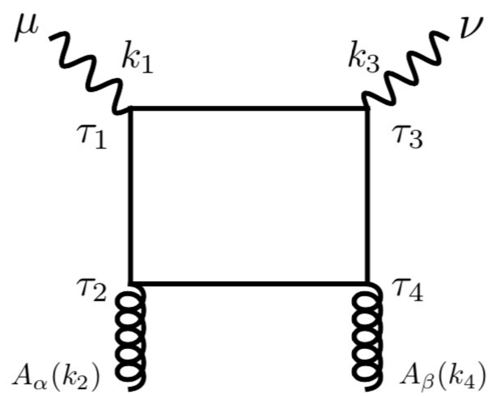

DIS with worldlines:
Tarasov, RV, 1903.11624,
2008.08104, 2109.10370

$$g_1 \propto \Gamma_A^{\mu\nu}[k_1,k_3] = \int \frac{d^4k_2}{(2\pi)^4} \int \frac{d^4k_4}{(2\pi)^4}\, \Gamma_A^{\mu\nu\alpha\beta}[k_1,k_3,k_2,k_4]\ \mathrm{Tr_c}(\tilde{A}_\alpha(k_2)\tilde{A}_\beta(k_4))$$

Polarization tensor
(antisymmetric piece)

Box diagram

Using a powerful worldline formalism of the one loop effective action in QCD, we can compute the box diagram (with no kinematic approximations of internal variables) in both Bjorken limit ($Q^2 \to \infty, s \to \infty, x = \text{fixed}$) and the Regge limit ($x \to 0, s \to \infty, Q^2 = \text{fixed}$). The latter result is new

Finding triangles in boxes in Bjorken and Regge asymptotics

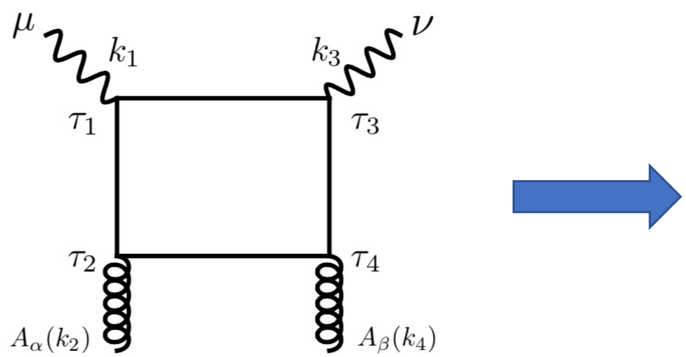

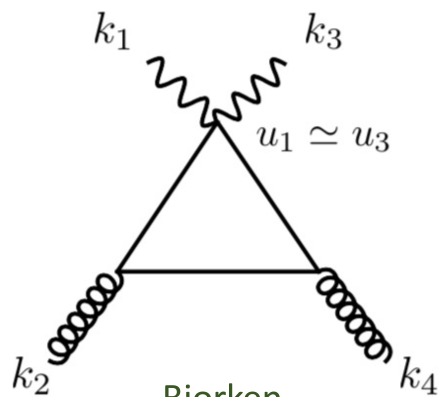

Bjorken

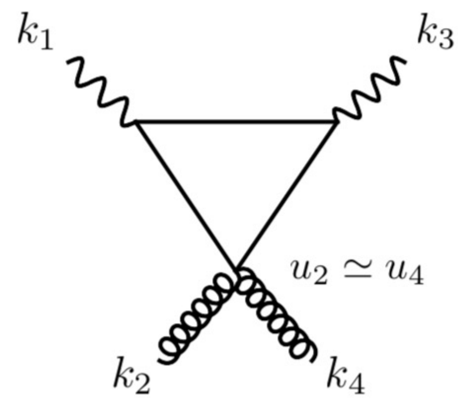

Regge

Tarasov, RV, arXiv:2008.08104

Remarkably, box diagram for $g_1(x_B,Q^2)$ has same structure in both limits, dominated by the triangle anomaly !

$$S^\mu g_1(x_B,Q^2)\Big|_{Q^2\to\infty} = \sum_f e_f^2 \frac{\alpha_s}{i\pi M_N}\int_{x_B}^1 \frac{dx}{x}\left(1-\frac{x_B}{x}\right)\int \frac{d\xi}{2\pi}e^{-i\xi x}\lim_{l_\mu\to 0}\frac{l^\mu}{l^2}\langle P',S|\mathrm{Tr}_c F_{\alpha\beta}(\xi n)\tilde{F}^{\alpha\beta}(0)|P,S\rangle + \text{non-pole}\ \frac{\Lambda^2_{QCD}}{Q^2} << 1$$

$$S^\mu g_1(x_B,Q^2)|_{x_B\to 0} = \sum_f e_f^2 \frac{\alpha_s}{i\pi M_N}\int_{x_B}^1 \frac{dx}{x}\int \frac{d\xi}{2\pi}e^{-i\xi x}\lim_{l_\mu\to 0}\frac{l^\mu}{l^2}\langle P',S|\mathrm{Tr}_c F_{\alpha\beta}(\xi n)\tilde{F}^{\alpha\beta}(0)|P,S\rangle + \text{non-pole}\ \frac{x_B}{x} << 1$$

Hence g_1 is topological in both asymptotic limits of QCD…it has no relation to $\Delta g(x,Q^2)$

Finding triangles in boxes in Bjorken and Regge asymptotics

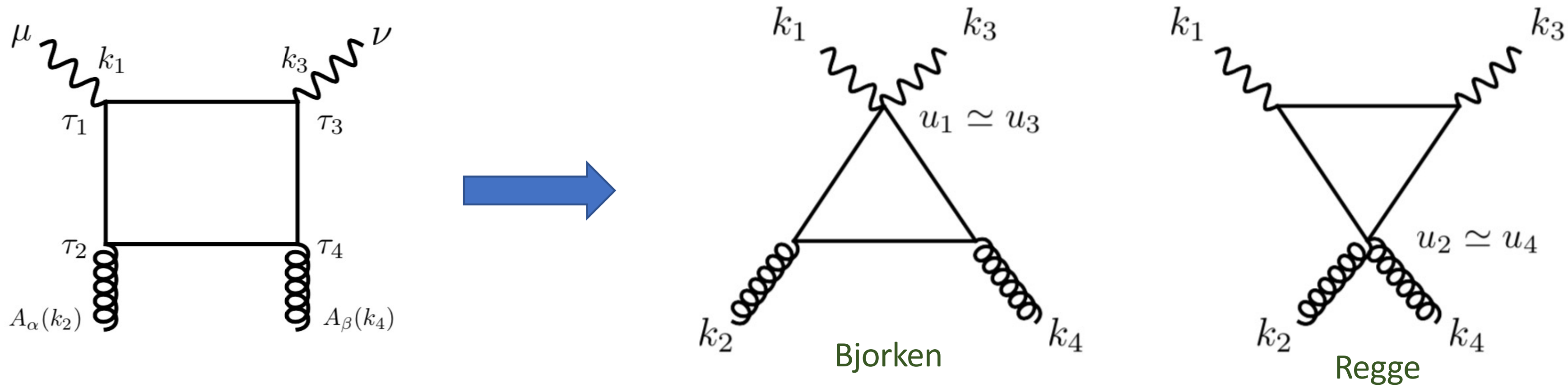

Tarasov, RV, arXiv:2008.08104

$$\frac{1}{4\pi^2}\frac{l^\kappa}{l^2}\int\frac{d^4k_2}{(2\pi)^4}\int\frac{d^4k_4}{(2\pi)^4}\,\mathrm{Tr}_c F_{\alpha\beta}(k_2)\tilde{F}^{\alpha\beta}(k_4)\,(2\pi)^4\delta^4(l+k_2+k_4)$$

What happens then to the anomaly pole ? There cannot be such an infrared divergence in QCD !

The resolution of this question resolves simulataneously two key ”puzzles:

The $U_A(1)$ problem, or why is the η' meson so massive ?
Why the proton’s helicity is much smaller than that predicted the Ellis-Jaffe sum rule

A big role for a phase: the WZW isosinglet term

Tarasov,Venugopalan, arXiv:2109.10370

$$S^{\bar{\eta}}_{\mathrm{WZW}} = -i\frac{\sqrt{2n_f}}{F_{\bar{\eta}}}\int d^4x\,\bar{\eta}\,\Omega$$

Ω is the topological charge density and F_η is the η' decay constant

This term can be derived explicitly from the imaginary part of W_I

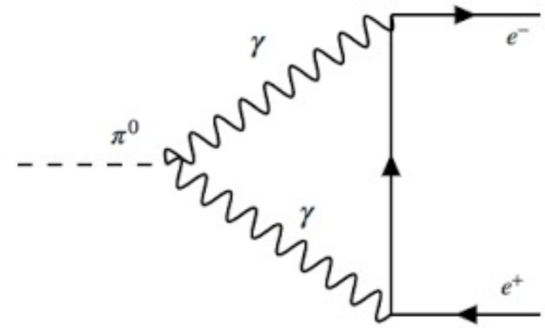

Another famous WZW term is that responsible for $\pi^0 \rightarrow 2\,\gamma$

This corresponds to the anomaly in the isotriplet axial vector current

$$\langle P', S|J_5^\mu|P, S\rangle = \bar{u}(P', S)\Big[\gamma^\mu\gamma_5 G_A(l^2) + l^\mu\gamma_5 G_P(l^2)\Big]u(P, S)$$

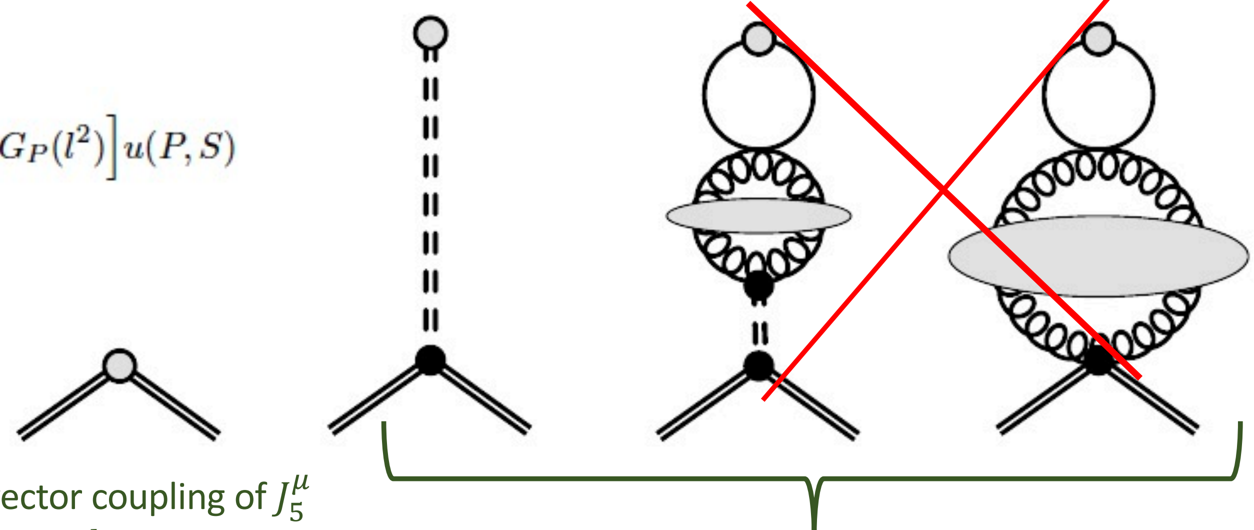

Direct axial vector coupling of J_5^μ to polarized proton

Pseudoscalar coupling of polarized proton to J_5^μ

Goldberger-Treiman relation

$$\langle P', S | J_5^\mu | P, S\rangle = \bar{u}(P', S)\Big[\gamma^\mu \gamma_5 G_A(l^2) + l^\mu \gamma_5 G_P(l^2)\Big] u(P, S)$$

Veneziano (1989)

Anomalous Goldberger-Treiman relation

$$G_A(0) = \frac{\sqrt{2\tilde{n}_f}}{2M_N} F_{\bar{\eta}}\, g_{\eta_0 NN}$$

$g_{\eta_0 \mathrm{NN}}$ represents the coupling
of the isosinglet field to the proton

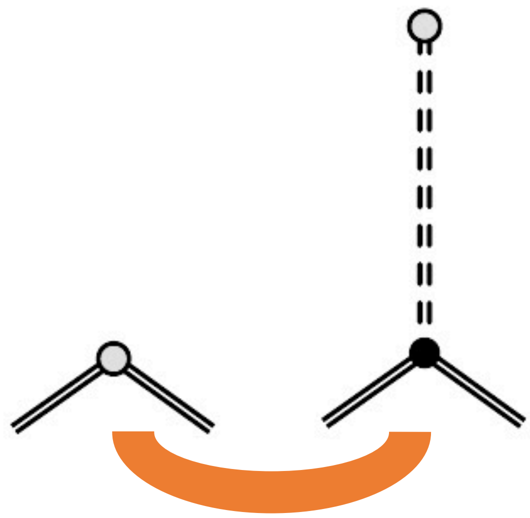

The anomaly equation and the absence of a pole in G_P relates the axial vector and pseudoscalar sectors

This underlines our understanding of the “primordial” $\bar{\eta}$
as the isosinglet Goldstone boson of the pseudoscalar $U_V(3)$ nonet
- the anomaly breaks $U_A(1)$ endowing the $\bar{\eta}$ with a mass: $\bar{\eta} \to \eta'$

The role of the Yang-Mills topological susceptibility

Absence of a pole in
the pseudoscalar formfactor
also implies…

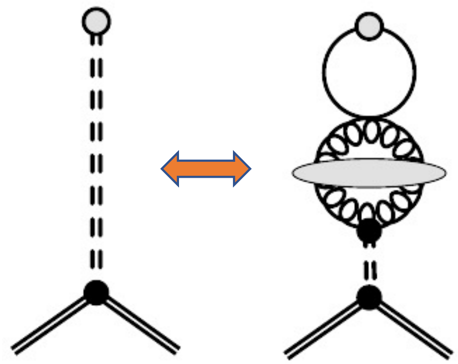

$$\chi(l^2) = i\int d^4x\, e^{ilx}\langle 0|T\,\Omega(x)\Omega(0)|0\rangle$$

1/N corrections to the YM susceptibility
induced by the WZW coupling
generate the QCD top. susceptibility

$$\chi(l^2) = l^2 \frac{1}{l^2 - m_{\eta'}^2}\chi_{\rm YM}(l^2) \quad \text{with} \quad m_{\eta'}^2 \equiv -\frac{2n_f}{F_{\bar\eta}^2}\chi_{\rm YM}(0)$$

Witten-Veneziano formula

$\chi(l^2) \to 0 \; when \; l^2 \to 0$

These relations fundamentally explain both
the $U_A(1)$ puzzle and the“spin crisis”

What about g_1 at small x_{Bj}

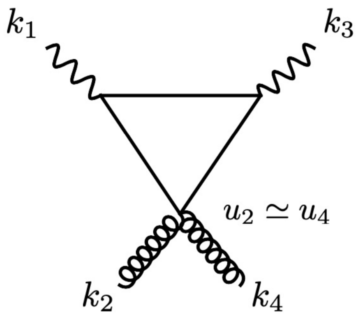

Regge

g_1 in the Regge limit is also controlled by the anomaly

How does gluon saturation influence the anomaly ?

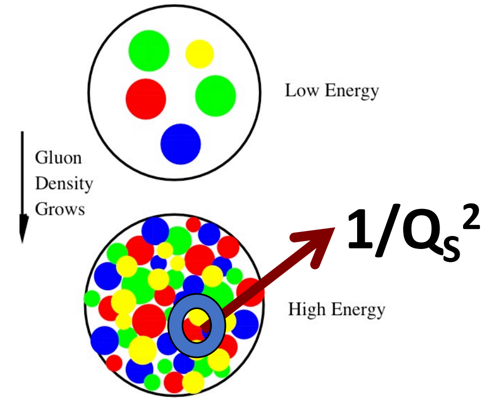

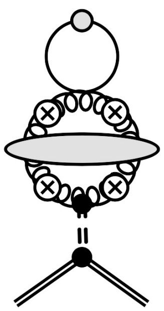

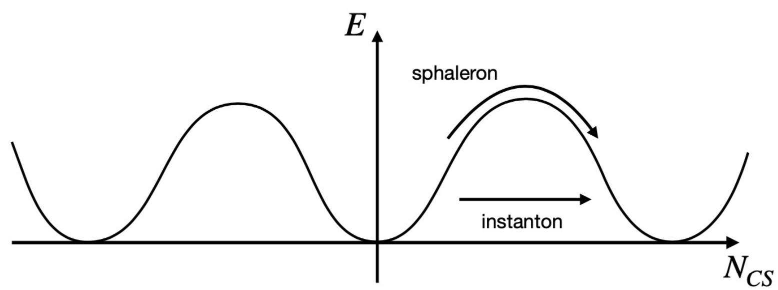

Gluon saturation induces over the barrier sphaleron-like transitions

Tarasov,Venugopalan, arXiv:2109.10370

What about g_1 at small x_{Bj} ?

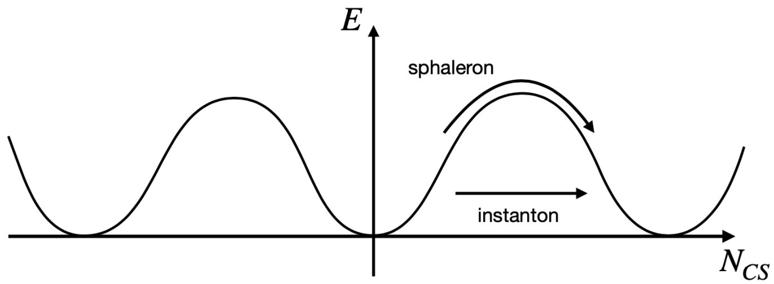

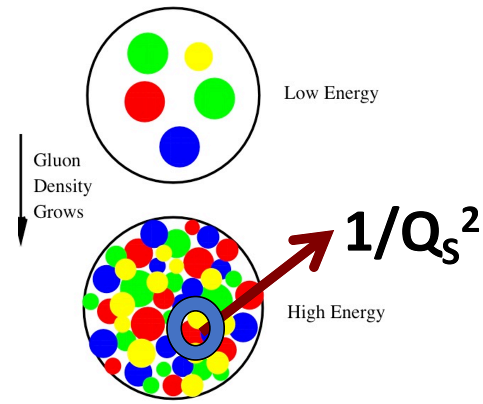

Gluon saturation induced over the barrier sphaleron-like transitions estimated by an axion-like effective action and its coupling to the CGC

$$g_1^{\text{Regge}}(x_B,Q^2) = \left(\sum_f e_f^2\right)\frac{n_f\alpha_s}{\pi M_N} i\int d^4y \int_{x_B}^1 \frac{dx}{x}\left(1-\frac{x_B}{x}\right)\int\frac{d\xi}{2\pi}e^{-i\xi x}\int\mathcal{D}\rho\, W_Y[\rho]\int D\bar{\eta}\,\tilde{W}_{P,S}[\bar{\eta}]\int[DA]$$

$$\times\,\mathrm{Tr}_c F_{\alpha\beta}(\xi n)\tilde{F}^{\alpha\beta}(0)\,\eta_0(y)\,\exp\left(iS_{\text{CGC}}+i\int d^4x\left[\frac{1}{2}\left(\partial_\mu\bar{\eta}\right)\left(\partial^\mu\bar{\eta}\right)-\frac{\sqrt{2n_f}}{F_{\bar{\eta}}}\bar{\eta}\,\Omega\right]\right)$$

Can be studied it two limits: $Q_S^2 < m_{\eta'}^2$ and $Q_S^2 > m_{\eta'}^2$

Tarasov,Venugopalan, arXiv:2109.10370

What about g_1 at small x_{Bj} ?

For $Q_S^2 < m_{\eta'}^2$,
over the barrier transition

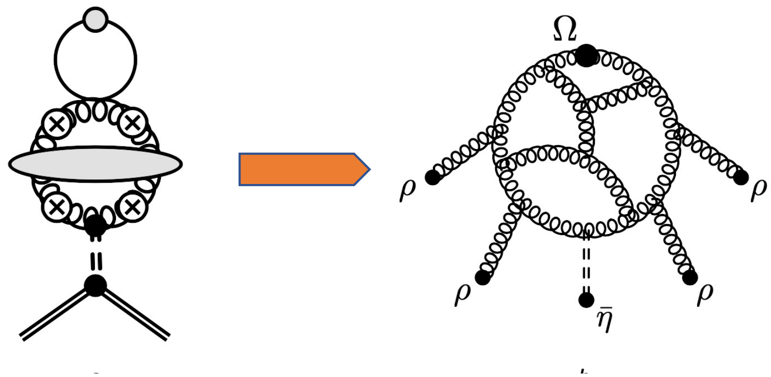

Spin diffusion due to “drag force” on “axion” propagation in the shock wave background
-drag force is proportional to sphaleron transition rate

McLerran,Mottola,Shaposhnikov (1990)

$$g_1^{\rm Regge}(x_B, Q^2) \propto \frac{Q_S^2 m_{\eta'}^2}{F_{\bar\eta}^3 M_N} \exp\left(-4\, n_f C\, \frac{Q_S^2}{F_{\bar\eta}^2}\right)$$

Very rapid quenching of spin diffusion at small x_{Bj} !

Tarasov,Venugopalan, arXiv:2109.10370

What about g_1 at small x_{Bj} ?

For $Q_S^2 \;>\; m_{\eta'}^2$,
axion is perturbation
to shock wave background

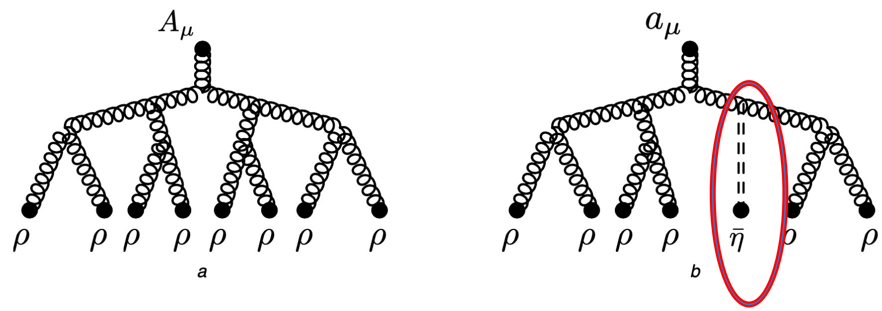

Calculation analogous to calculation of axion dynamics in the Glasma

Jokela, Kajantie, and Sarkkinen, arXiv:2012.14160 [hep-ph]

Estimate also gives exponential suppression with increasing Q_S – prefactors remain to be worked out

Tarasov,Venugopalan, arXiv:2109.10370

Thank you for your attention !